iScience

CellPress
OPEN ACCESS

Article

Photocage-Selective Capture and Light-Controlled Release of Target Proteins

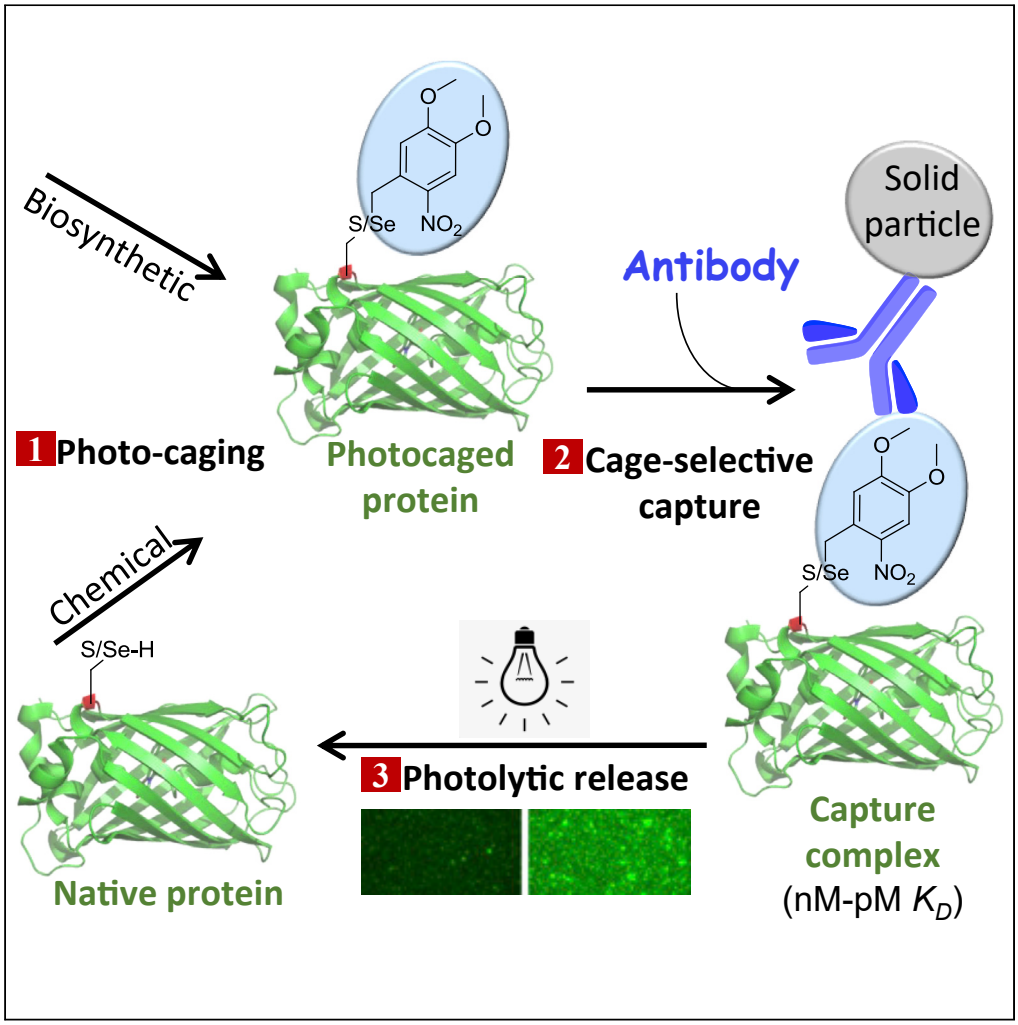

Rasa Rakauskaitė, Giedrė Urbanavičiūtė, Martynas Simanavičius, ..., Viktoras Masevičius, Aurelija Žvirblienė, Saulius Klimašauskas

saulius.klimasauskas@bti.vu.lt

HIGHLIGHTS

The first high-affinity monoclonal antibody specific for a popular photocaging group

A new tool for selective detection of DMNB-tagged proteins in complex mixtures

Enables non-covalent capture of native proteins with surface-exposed DMNB groups

Orthogonal protein manipulation by photocage-selective capture and photolytic release

Rakauskaitė et al., iScience 23, 101833
December 18, 2020
https://doi.org/10.1016/j.isci.2020.101833

iScience

CellPress
OPEN ACCESS

Article

Photocage-Selective Capture and Light-Controlled Release of Target Proteins

Rasa Rakauskaitė,[1,3] Giedrė Urbanavičiūtė,[1,3] Martynas Simanavičius,[1] Rita Lasickienė,[1] Aušra Vaitiekaitė,[1] Gražina Petraitytė,[1,2] Viktoras Masevičius,[1,2] Aurelija Žvirblienė,[1] and Saulius Klimašauskas[1,4,*]

SUMMARY

Photochemical transformations enable exquisite spatiotemporal control over biochemical processes; however, methods for reliable manipulations of biomolecules tagged with biocompatible photo-sensitive reporters are lacking. Here we created a high-affinity binder specific to a photolytically removable caging group. We utilized chemical modification or genetically encoded incorporation of noncanonical amino acids to produce proteins with photocaged cysteine or selenocysteine residues, which were used for raising a high-affinity monoclonal antibody against a small photoremovable tag, 4,5-dimethoxy-2-nitrobenzyl (DMNB) group. Employing the produced photocage-selective binder, we demonstrate selective detection and immunoprecipitation of a variety of DMNB-caged target proteins in complex biological mixtures. This combined orthogonal strategy permits photocage-selective capture and light-controlled traceless release of target proteins for a myriad of applications in nanoscale assays.

INTRODUCTION

Optical control of protein function enables an exquisite spatial and temporal interrogation of biological processes that cannot be accomplished with other conditional control elements. This is often achieved by using photolabile protecting groups (caging groups); removal of these caging groups by light (decaging) is a mild and noninvasive technique that is completely orthogonal to other chemical processes in a biological system. This approach has been successfully applied for photochemical control of the activity of small molecules, peptides, oligonucleotides, and proteins (Ankenbruck et al., 2018; Dumas et al., 2015; Shimizu et al., 2006; Spicer and Davis, 2014).

Installation of photocaging groups in biomolecules can be achieved by (1) chemical or chemo-enzymatic modification of native biopolymers or (2) incorporation of caged monomers during *de novo* chemical or enzymatic assembly of biopolymers (typically for oligonucleotides and oligopeptides). For proteins, systems for biosynthetic incorporation of photocaged lysine, tyrosine, serine, cysteine, and selenocysteine residues have been described (Riggsbee and Deiters, 2010). In particular, a high nucleophilicity of the thiol moiety in cysteine residues has long been used for installing a wide variety of functionalities (Chalker et al., 2009). Cys has a relatively low natural abundance, and solvent-exposed free cysteines are rather uncommon in wild-type proteins. An even more unique and powerful functionality in proteins is endowed by the 21st amino acid, selenocysteine (Arnér, 2010). A few strategies for efficient biosynthesis of proteins containing photocaged Cys or Sec residues at genetically predetermined positions have recently been proposed (Lemke et al., 2007; Nguyen et al., 2014; Peeler et al., 2020; Rakauskaitė et al., 2015; Uprety et al., 2014). The 4,5-dimethoxy-2-nitrobenzyl (DMNB) caging group shields highly reactive Sec (or solvent exposed Cys) from undesired side reactions inside producing cells and during subsequent manipulations and can be readily removed by illumination with 365 nm light (Shao and Xing, 2010). However, isolation of DMNB-caged proteins or their manipulations *in vitro* or inside cells requires additional tags or the development of individual protocols for each new protein since no affinity ligands are known to specifically interact with this relatively small moiety.

To expand the general applicability and functional capability of this technology, we went on to develop a non-covalent binder that is specific toward this small chemical group (Figure 1). This was achieved by

[1]Institute of Biotechnology, Life Sciences Center, Vilnius University, LT-10257 Vilnius, Lithuania

[2]Institute of Chemistry, Department of Chemistry and Geosciences, Vilnius University, LT-10257 Vilnius, Lithuania

[3]These authors contributed equally

[4]Lead Contact

*Correspondence: saulius.klimasauskas@bti.vu.lt

https://doi.org/10.1016/j.isci.2020.101833

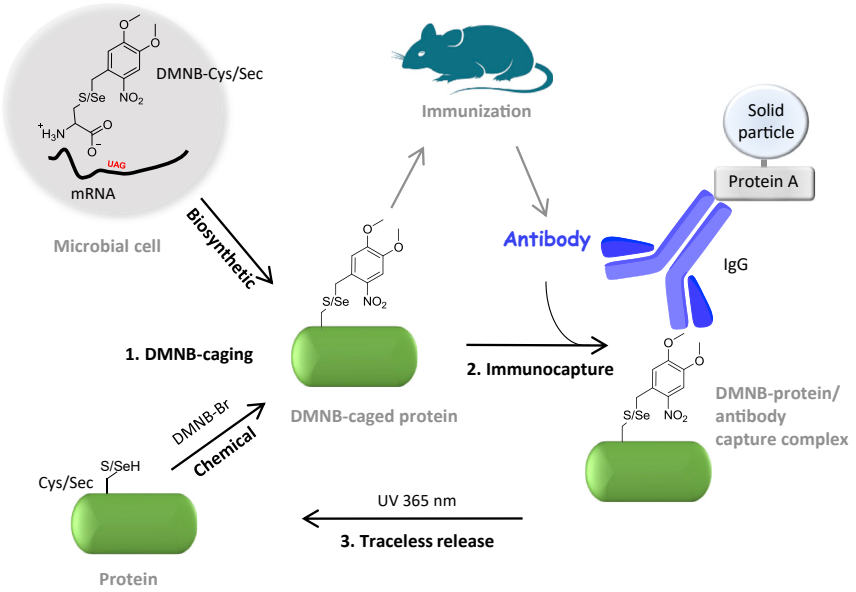

Figure 1. Selective Capture and UV Light-Controlled Traceless Release of Proteins Containing a Biosynthetically or Chemically Incorporated Photosensitive Caging Group Using a DMNB-Selective Monoclonal Antibody

raising a monoclonal antibody against a chemically DMNB-modified carrier protein in mice. Detailed characterization of the produced selective binder demonstrated its utility for selective analysis and targeted manipulation of chemically and biosynthetically DMNB-caged proteins.

RESULTS AND DISCUSSION

Production and Evaluation of Monoclonal Antibodies

The DMNB group falls in a category of very small haptens (<300 Da), which are incapable of inducing a sufficient immune response required for antibody production (Chappey et al., 1994). To increase the immunogenicity, the hapten was covalently coupled to the KLH carrier protein, a well-established immunogen. KLH-DMNB conjugates were produced by direct chemical derivatization of accessible (predominantly) Cys residues with DMNB bromide. Alternatively, to increase the number of reactive –SH groups, KLH was first treated with a sulfhydryl-addition reagent, SATA (*N*-succinimidyl-*S*-acetylthioacetate), deacylated with hydroxylamine and then conjugated with DMNB resulting in a KLH-AT-DMNB conjugate (Figure S1). This conjugate was used to immunize mice, whereas similarly prepared BSA-DMNB and BSA-AT-DMNB conjugates were used to evaluate the specificity of the antibodies. The BSA-DMNB and BSA-AT-DMNB conjugates contained a mixture of proteins carrying 1–3 DMNB or 5–12 ATA groups (determined after first reaction with SATA), respectively (Figures S2 and S3).

Hybridoma cell lines for anti-DMNB monoclonal antibody production were created using BALB/c mice. A total of eight DMNB-positive clones were selected, multiplied, and stabilized by recloning. All hybridomas produced MAbs of IgG class (Table S1). The specificity and affinity of the antibodies was evaluated by an ELISA immunoassay using the immunization antigen KLH-AT-DMNB as well as unrelated conjugates BSA-DMNB and BSA-AT-DMNB (Table S1; see Table S2 for derivatized proteins details). Of eight selected hybridomas, seven produced DMNB-specific MAbs that interacted only with DMNB-proteins but not with the carrier proteins (Figure S4). The apparent dissociation constants of DMNB-specific MAbs were in the low nanomolar to picomolar range indicating a high affinity toward the antigens. We selected the best behaved monoclonal antibody of IgG2a subclass (clone 12B6 in Figure S4, further referred to as Photo Cage Selective Binder, PCSB), which afforded excellent interaction with bacterial Protein A and thus permitted facile coupling to accessory components such as proteins or solid particles (Figure 1).

Robust interactions of PCSB observed in immunoassays (Figure S5) were further confirmed by western blot analyses. PCSB not only bound KLH and BSA proteins carrying multiple DMNB groups but also was sensitive at more stringent conditions—identifying the biosynthetic EGFP Y39C-DMNB protein (see Table S3 for

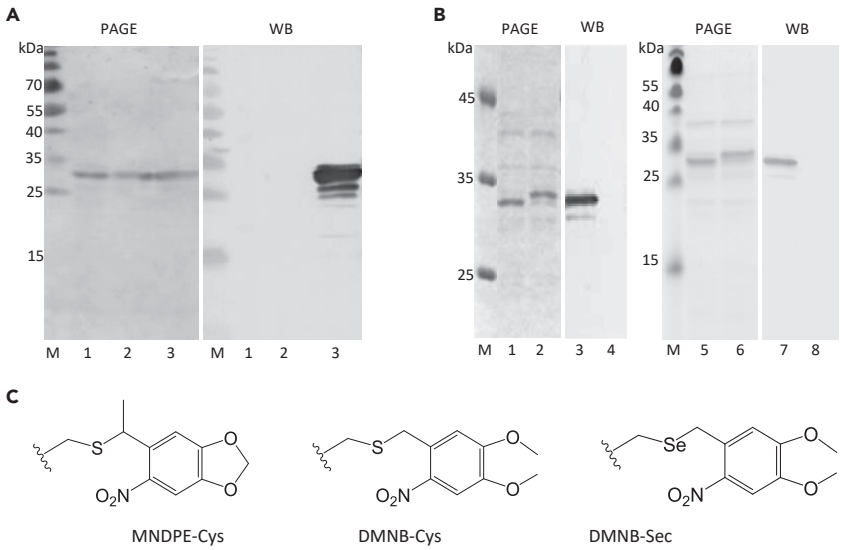

Figure 2. Selective Detection of Biosynthetic Photocaged EGFP Y39X Proteins with PCSB

(A) Selectivity of PCSB toward the MNDPE and DMNB caging groups. EGFP Y39X protein samples were fractionated by electrophoresis in SDS-PA gels and were Coomassie stained (PAGE, left) or analyzed by western blotting using PCSB (WB, right). Lane 1, X = MNDPE-Cys; lane 2, X = Leu/Ile; lane 3, X = DMNB-Cys; M, protein size marker.

(B) Selectivity of PCSB toward photocaged Cys and Sec residues. EGFP Y39X protein samples were fractionated by electrophoresis in SDS-PA gels and were Coomassie stained (PAGE) or analyzed by western blotting using PCSB (WB). Lanes 1, 3, X = DMNB-Cys; lanes 2, 4, X = DMNB-Cys illuminated with UV; lanes 5, 7, X = DMNB-Sec; lanes 6, 8, X = DMNB-Sec illuminated with UV; M, protein size marker.

(C) Structures of the caged residues MDNPE-Cys, DMNB-Cys, and DMNB-Sec.

recombinant constructs details) labeled with a unique DMNB group (Figure 2A). Remarkably, in these experiments PCSB was able to discriminate against a chemically similar 4,5-(methylenedioxy)-2-nitrophenyl) ethyl (MDNPE) group (Figures 2A and 2C). Further western blot analyses revealed that PCSB interacted with the antigen irrespective of whether the DMNB protecting group was attached to a S or Se atom in EGFP Y39C-DMNB and EGFP Y39U-DMNB proteins, respectively. These interactions were lost when DMNB groups were removed from the proteins upon 365 nm light exposure (Figure 2B). Using western blotting of serial dilutions of purified proteins, we determined the detection limits to be 16 ng for BSA-$(DMNB)_{1-3}$, 31 ng for EGFP N150C-DMNB, and 63 ng for SUMOstar E89C-DMNB (Figure S6). Altogether, these data indicate that the generated PCSB performed as a highly sensitive and selective tool suitable for DMNB group recognition.

Detection and Capture of Photocaged Proteins

To explore the capacity of PCSB to detect DMNB-caged proteins in complex biological mixtures, we expanded the repertoire of model proteins by including three well-studied bacterial DNA cytosine-5 methyltransferases: M.HhaI, M.HpaII, and M2.Eco31I. These medium-sized proteins use their essential catalytic Cys residues to facilitate the transmethylation of target cytosine residues and can be engineered to deposit larger chemical moieties to DNA (Lukinavičius et al., 2012).

Biosynthetic expression of these recombinant proteins, produced in a photocaged and thus catalytically mute form (SUMOstar-M.HhaI C81C-DMNB, SUMOstar-M.HpaII C103C-DMNB, SUMOstar-M2.Eco31I C232C-DMNB), was monitored by western blot analysis of total yeast cell lysates (Figure S7). As expected, DMNB-positive blot signals were observed only in samples containing the expressed recombinant proteins carrying the DMNB-Cys residue but showed no interaction with controls expressing non-caged protein variants (containing Leu or Ile residues) or samples prepared from uninduced cells.

Next, we checked if the interaction between the small DMNB group and the PCSB was sufficiently high to allow manipulations of native proteins by immunoprecipitation (IP) in solution. For this purpose, we first used chemically labeled DMNB-proteins carrying multiple DMNB groups to form immunoprecipitation

complexes on Sepharose-Protein A beads preincubated with PCSB. The composition of the resulting IP complexes was revealed by western blot analysis of the denatured extractions of IP suspensions fractionated using gel electrophoresis. Both model methyltransferases M.HpaII-$(DMNB)_{1-5}$ and M2.Eco31I-$(DMNB)_{\geq 2}$ proteins were equally well immunoprecipitated from their pure solutions as well as from complex molecular mixtures that were prepared by adding chemically labeled DMNB-protein preparation to a total yeast cell lysate (Figure S8). Control IP reactions indicated that unlabeled recombinant proteins, components of yeast cell lysate, or unrelated isotypic MAbs showed no interference during IP. Similarly, several mutant variants of chemically labeled EGFP-DMNB and SUMOstar-DMNB proteins were found to be able to form the IP complexes (Figure S9).

Further, we performed IP experiments using a series of biosynthetic recombinant protein variants each caged with a single DMNB group incorporated at a genetically defined position. Three of five analyzed EGFP-DMNB protein variants and three of four SUMOstar-DMNB protein variants showed a high or very high IP efficiency (Figures 3A and 3B). Moreover, we were able to isolate the expressed SUMOstar I106DMNB-C protein out of the yeast cell lysate (Figure 3C). These data indicate that a single DMNB group sufficiently exposed on a surface of a native protein can be used for manipulating the latter using the generated PCSB.

A brief irradiation with UV light leads to photolysis of the DMNB caging group releasing a cage-free target protein from the IP complex. A light controlled release of a chemically caged EGFP D117C$(DMNB)_{1-3}$ protein from an IP complex was observed as reduction of fluorescence intensity on beads and simultaneous increase of fluorescence intensity in solution (Figures 4A–4C). SDS-PAGE, HPLC-ESI/MS, and western blot analysis of the reaction showed the expected size of the EGFP D117C protein in solution (Figures 4D and 4E). Analogous results were obtained with a chemically caged SUMOstar I106C-$(DMNB)_{1-2}$ protein (Figure S10) and biosynthetic single-label SUMOstar I106C-DMNB protein extracted from a yeast cell lysate (Figures 4D and 4F). In the latter case, Ni^{++} affinity chromatography of biosynthetic SUMOstar I106C-DMNB from yeast cells showed that a prevailing fraction of the produced protein was truncated at the antepenultimate position (SUMOstar105ter, residues 1–105) (Figure 4F, top panel). Remarkably, during the IP procedure, only the full length protein (residues 1–108) has been effectively pulled out from a dilute cell lysate and photolytically recovered in a pure label-free form with no detectable amounts of the contaminating SUMOStar105ter variant (Figure 4F, bottom panel).

DISCUSSION

Here we report the development of the first highly selective non-covalent binder for a popular photocaging group that can be biosynthetically incorporated into recombinant proteins in yeast (Lemke et al., 2007; Rakauskaitė et al., 2015) and mammalian (Nguyen et al., 2014; Peeler et al., 2020) cells or installed *de novo* by chemical or chemoenzymatic labeling (Anhäuser et al., 2018; Heimes et al., 2018). This new tool effectively expands the functionality of the photocaging moiety into a useful orthogonal affinity handle. Despite the small size of the target group, the present PCSB displays a high affinity (nM–pM) and specificity toward a range of DMNB-caged proteins and permits selective determination of nanogram quantities of target proteins or analysis of DMNB-proteomes in biological milleux by western blotting. Consistent with the relative bulkiness of the antibody Fab region (Chiu et al., 2019), we found that binding of the DMNB group in native proteins was strongly dependent on its accessibility. However, for both model systems examined, multiple surface positions were identified that permitted selective PCSB capture of biosynthetically produced or chemically modified proteins (Figure 3). In light of a growing interest in optogenetics (Guglielmi et al., 2016) and nucleic acids-based nanodevices (Chakraborty et al., 2016), it will be attractive to determine the PCSB accessibility of DMNB groups located in single-stranded oligonucleotides and double stranded DNA/RNA structures. The presented series of examples demonstrates the first general approach in which a selective capture and traceless release of a caged protein can be achieved in a light-controlled fashion under near physiological non-denaturating conditions (Figures 4 and S10). Such tools are highly desirable for laboratory production of designer proteins, or even less accessible selenoproteins, and expand the availability and diversity of functionalized biomolecules for applications in miniature light-controlled systems involving microfluidic devises, microchips, and nanoparticles (Yang et al., 2017; Young and Schultz, 2018; Khamo et al., 2017; Silva et al., 2019; Sortino, 2012).

Limitations of the Study

Immunocapture of native proteins is limited to those that carry surface-exposed DMNB groups. On the other hand, PCSB interactions with SDS-denatured proteins during western blot analyses proved effective

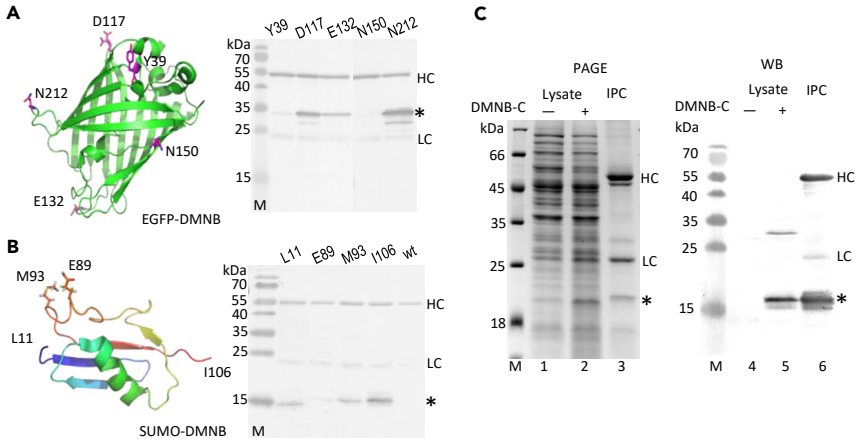

Figure 3. Immuno-Capture of Recombinant EGFP and SUMOstar Variants Containing a Biosynthetically Incorporated Unique DMNB-Cys Residue

(A) EGFP-DMNB variants purified from yeast cells were immunoprecipitated using MagnaBind-Protein A beads preincubated with PCSB. Shown is a protein model indicating positions of incorporated DMNB-Cys residues (left) and IP complexes resolved on a SDS-PA gel and analyzed by western blotting using PCSB (right).

(B) SUMO-DMNB variants purified from yeast cells were processed as described above. Shown is a protein model indicating positions of incorporated DMNB-Cys residues (left) and IP complexes analyzed by western blotting using PCSB as above (right).

(C) Immunoprecipitation of biosynthetic protein SUMOstar I106C-DMNB from yeast cell lysate. A total extract from cells not expressing (lanes 1, 4) and expressing (lanes 2, 5) target protein as well as IP complex assembled using the latter cell lysate (lanes 3, 6) was fractionated in SDS-PA gel (left panel) or analyzed by western blotting using PCSB (right panel). Bands of the target proteins are indicated by asterisks. HC, heavy chain; LC, light chain; IPC, immunoprecipitation complex; M, protein size marker.

independently of their tag location. Photochemical decaging using UV light is known to generate free radicals and reactive oxygen species, which may be detrimental to native proteins and other macromolecules Kerwin and Remmele, 2007. Therefore, inclusion of radical/oxygen scavenging compounds such as methionine in reaction buffers and use of inorganic material-based solid particles for assembly of IP complexes is advised.

Resource Availability

Lead Contact

Further information and requests for resources and reagents should be directed to and will be fulfilled by the Lead Contact, Saulius Klimašauskas (saulius.klimasauskas@bti.vu.lt).

Materials Availability

Plasmids generated in this study will be made available upon request.

The antibody generated in this study will be made available on request, but we may require a payment and/or a completed Materials Transfer Agreement.

Data and Code Availability

This study did not generate datasets or codes.

METHODS

All methods can be found in the accompanying Transparent Methods supplemental file.

SUPPLEMENTAL INFORMATION

Supplemental Information can be found online at https://doi.org/10.1016/j.isci.2020.101833.

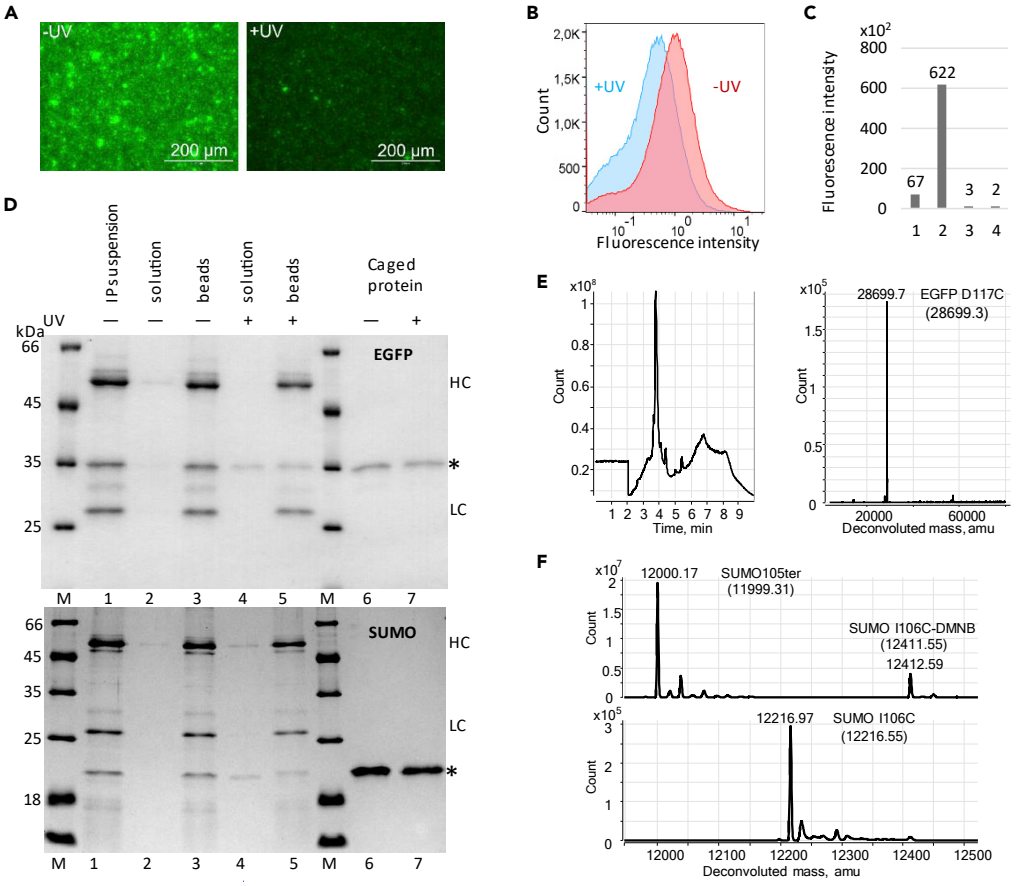

Figure 4. Immunocapture and Light-Controlled Release of DMNB-Caged Proteins

(A) Fluorescence imaging of IP complexes (Silica bead-Protein A/PCSB/EGFP D117C-$(DMNB)_{1-3}$) before (left) and after (right) 365 nm light exposure.

(B) Flow cytometry analysis of IP complexes (Silica bead-Protein A/PCSB/EGFP D117C-$(DMNB)_{1-3}$) before and after 365 nm light exposure.

(C) EGFP fluorescence in solution upon UV treatment of IP complexes. Suspensions of IP complexes (Silica bead-Protein A/PCSB/EGFP D117C-$(DMNB)_{1-3}$, lanes 1, 2) and control complexes (Silica bead-Protein A/PCSB/EGFP D117C, lanes 3, 4) were either not exposed (lanes 1,3) or exposed (lanes 2, 4) to 365 nm light, after which beads were removed from solution.

(D) Photorelease of label-free EGFP D117C (top panel) and SUMOstar I106C (bottom panel) proteins. Pure protein solution or yeast cell lysate was used to immunoprecipitate the EGFP D117C-$(DMNB)_{1-3}$, and SUMOstar I106C-DMNB proteins, respectively. The DMNB-proteins were captured on silica-protein A beads containing PCSB (lane 1). Control (lanes 2, 3) and illuminated samples (lanes 4, 5) to 365 mn light, after which the beads and solution were separated, fractionated in SDS-PA gel and visualized by Coomassie staining. Control photochemical reactions contained only pure EGFP D117C-$(DMNB)_{1-3}$ (top panel) or SUMOstar I106C-$(DMNB)_{1-2}$ (bottom panel, lanes 6, 7). Bands of the target proteins are indicated by asterisks. HC, heavy chain; LC, light chain; M, protein size marker.

(E) HPLC-ESI/MS identification of the label-free photolytically released EGFP D117C protein (lane 4 in D). +ESI TIC time course of the released protein (left panel) and deconvoluted MS of its 3.58–3.84 min peak (right panel).

(F) Biosynthetic production of N-terminally His-tagged SUMOstar I106C-DMNB protein. MS analysis of Ni-IMAC purified protein (top panel) revealed a mixture of full length (SUMO I106C-DMNB) and truncated (residues 1–105, SUMO 105ter) variants. Immunocapture and photochemical release of SUMOstar (bottom panel) from the cell lysate (lane 4 in D) yielded a full-length uncaged protein (SUMO I106C). Calculated masses are shown in parentheses.

ACKNOWLEDGMENTS

The authors thank Audronė Rukšėnaitė for HPLC/ESI-MS data acquisition, Žilvinas Kožemekinas for assistance with preparation of MNDPE-Cys and Pranciškus Vitta for technical support with the LED light source. This work was supported by the Research Council of Lithuania (grant S-MIP-17-57 to S.K.) and Vilnius University Infrastructure Support Fund.

AUTHOR CONTRIBUTIONS

Conceptualization, S.K. and A.Ž.; Methodology, Investigation, and Validation, R.R., G.U., M.S., R.L., and A.V.; Resources, G.P. and V.M.; Data Curation, G.U.; Writing – Original draft, R.R., G.U., M.S., V.M., and S.K.; Writing – Review & Editing, R.R. and S.K; Supervision, S.K., A.Ž., and V.M.; Project Administration, R.R. and S.K.; Funding Acquisition, S.K.

DECLARATION OF INTERESTS

R.R., G.U., M.S., R.L., A.Ž., and S.K. are inventors on a related patent application.

Received: October 8, 2020
Revised: November 10, 2020
Accepted: November 16, 2020
Published: December 18, 2020

REFERENCES

Anhäuser, L., Muttach, F., and Rentmeister, A. (2018). Reversible modification of DNA by methyltransferase-catalyzed transfer and light-triggered removal of photo-caging groups. Chem. Commun. (Camb.) *54*, 449–451.

Ankenbruck, N., Courtney, T., Naro, Y., and Deiters, A. (2018). Optochemical control of biological processes in cells and animals. Angew. Chem. Int. Ed. *57*, 2768–2798.

Arnér, E.S. (2010). Selenoproteins-What unique properties can arise with selenocysteine in place of cysteine? Exp. Cell Res. *316*, 1296–1303.

Chakraborty, K., Veetil, A.T., Jaffrey, S.R., and Krishnan, Y. (2016). Nucleic acid–based nanodevices in biological imaging. Annu. Rev. Biochem. *85*, 349–373.

Chalker, J.M., Bernardes, G.J.L., Lin, Y.A., and Davis, B.G. (2009). Chemical modification of proteins at cysteine: opportunities in chemistry and biology. Chem. Asian J. *4*, 630–640.

Chappey, O., Debray, M., Niel, E., and Scherrmann, J.M. (1994). Association constants of monoclonal antibodies for hapten: heterogeneity of frequency distribution and possible relationship with hapten molecular weight. J. Immunol. Methods *172*, 219–225.

Chiu, M.L., Goulet, D.R., Teplyakov, A., and Gilliland, G.L. (2019). Antibody structure and function: the basis for engineering therapeutics. Antibodies *8*, 55.

Dumas, A., Lercher, L., Spicer, C.D., and Davis, B.G. (2015). Designing logical codon reassignment – Expanding the chemistry in biology. Chem. Sci. *6*, 50–69.

Guglielmi, G., Falk, H.J., and De Renzis, S. (2016). Optogenetic control of protein function: from intracellular processes to tissue morphogenesis. Trends Cell Biol *26*, 864–874.

Heimes, M., Kolmar, L., and Brieke, C. (2018). Efficient cosubstrate enzyme pairs for sequence-specific methyltransferase-directed photolabile caging of DNA. Chem. Commun. *54*, 12718–12721.

Kerwin, B.A., and Remmele, R.L., Jr. (2007). Protect from light: photodegradation and protein biologics. J. Pharm. Sci. *96*, 1468–1479, https://doi.org/10.1002/jps.20815.

Khamo, J.S., Krishnamurthy, V.V., Sharum, S.R., Mondal, P., and Zhang, K. (2017). Applications of optobiology in intact cells and multicellular organisms. J. Mol. Biol. *429*, 2999–3017.

Lemke, E.A., Summerer, D., Geierstanger, B.H., Brittain, S.M., and Schultz, P.G. (2007). Control of protein phosphorylation with a genetically encoded photocaged amino acid. Nat. Chem. Biol. *3*, 769–772.

Lukinavičius, G., Lapinaitė, A., Urbanavičiūtė, G., Gerasimaitė, R., and Klimašauskas, S. (2012). Engineering the DNA cytosine-5 methyltransferase reaction for sequence-specific labeling of DNA. Nucleic Acids Res. *40*, 11594–11602.

Nguyen, D.P., Mahesh, M., Elsässer, S.J., Hancock, S.M., Uttamapinant, C., and Chin, J.W. (2014). Genetic encoding of photocaged cysteine allows photoactivation of TEV protease in live mammalian cells. J. Am. Chem. Soc. *136*, 2240–2243.

Peeler, J.C., Falco, J.A., Kelemen, R.E., Abo, M., Chartier, B.V., Edinger, L.C., Chen, J., Chatterjee, A., and Weerapana, E. (2020). Generation of recombinant mammalian selenoproteins through genetic code expansion with photocaged selenocysteine. ACS Chem. Biol. *15*, 1535–1540.

Rakauskaitė, R., Urbanavičiūtė, G., Rukšėnaitė, A., Liutkevičiūtė, Z., Juškėnas, R., Masevičius, V., and Klimašauskas, S. (2015). Biosynthetic selenoproteins with genetically-encoded photocaged selenocysteines. Chem. Commun. *51*, 8245–8248.

Riggsbee, C.W., and Deiters, A. (2010). Recent advances in the photochemical control of protein function. Trends Biotechnol. *28*, 468–475.

Shao, Q., and Xing, B. (2010). Photoactive molecules for applications in molecular imaging and cell biology. Chem. Soc. Rev. *39*, 2835–2846.

Shimizu, M., Yumoto, N., and Tatsu, Y. (2006). Preparation of caged compounds using an antibody against the photocleavable protecting group. Anal. Biochem. *348*, 318–320.

Silva, J.M., Silva, E., and Reis, R.L. (2019). Light-triggered release of photocaged therapeutics - where are we now? J. Control. Release *298*, 154–176.

Sortino, S. (2012). Photoactivated nanomaterials for biomedical release applications. J. Mater. Chem. *22*, 301–318.

Spicer, C.D., and Davis, B.G. (2014). Selective chemical protein modification. Nat. Commun. *5*, 4740.

Uprety, R., Luo, J., Liu, J., Naro, Y., Samanta, S., and Deiters, A. (2014). Genetic encoding of caged cysteine and caged homocysteine in bacterial and mammalian cells. Chembiochem *15*, 1793–1799.

Yang, Y., Mu, J., and Xing, B. (2017). Photoactivated drug delivery and bioimaging. Wiley Interdiscip. Rev. Nanomed. Nanobiotechnol. *9*, e1408.

Young, D.D., and Schultz, P.G. (2018). Playing with the molecules of life. ACS Chem. Biol. *13*, 854–870.

iScience, Volume *23*

Supplemental Information

Photocage-Selective Capture and Light-Controlled Release of Target Proteins

Rasa Rakauskaitė, Giedrė Urbanavičiūtė, Martynas Simanavičius, Rita Lasickienė, Aušra Vaitiekaitė, Gražina Petraitytė, Viktoras Masevičius, Aurelija Žvirblienė, and Saulius Klimašauskas

Supplemental Figures

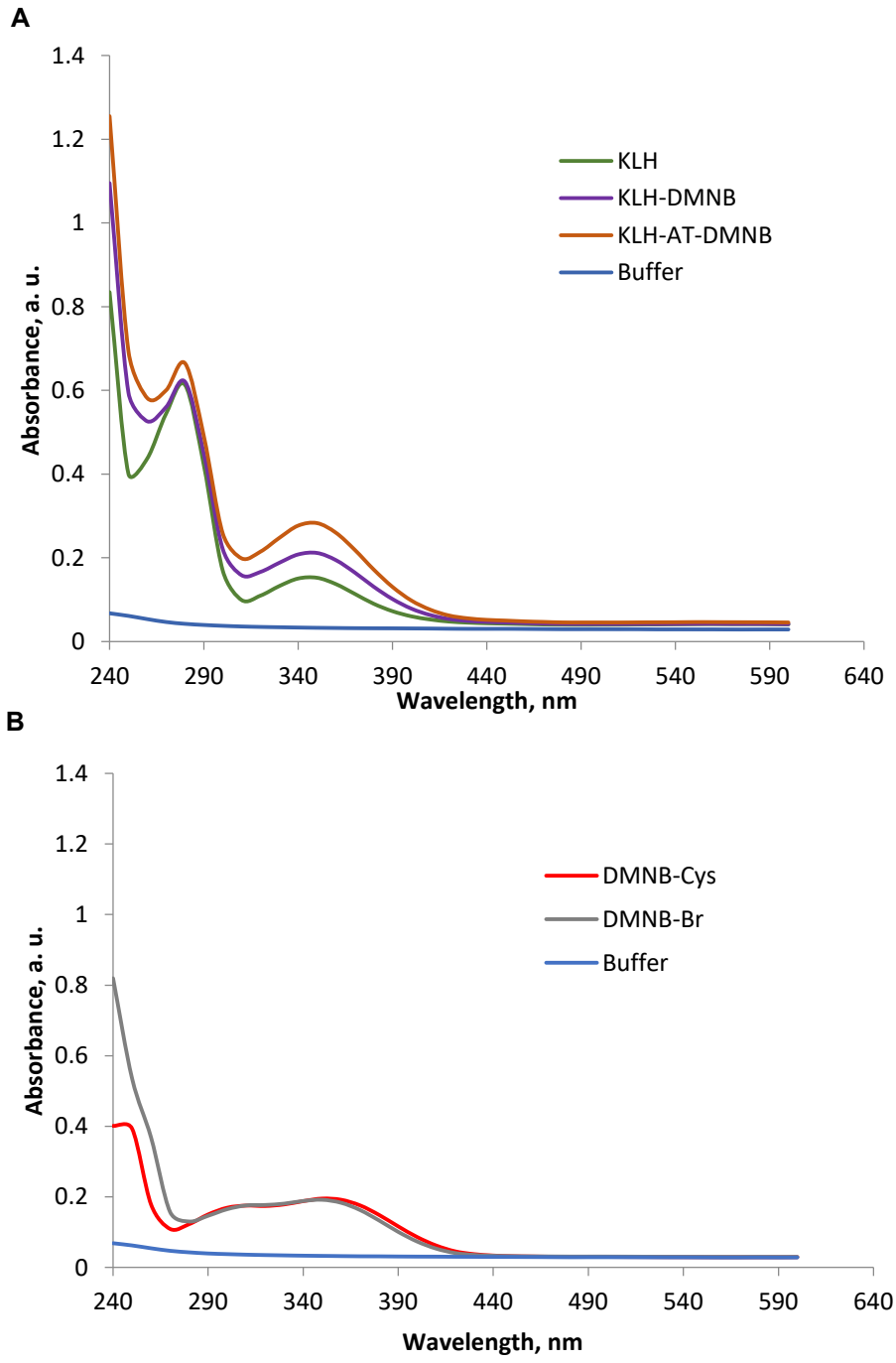

Figure S1. Spectrophotometric analysis of the immunization antigen (Related to Figure 1).
Absorbance spectra of original and chemically modified KLH proteins (A) and the DMNB-Cys/DMNB-Br precursors (B).
The KLH protein was treated with DMNB-Br directly or first conjugated with SATA reagent, deacetylated with hydroxylamine and then conjugated with DMNB-Br to produce the KLH-DMNB and KLH-AT-DMNB antigens, respectively. The extent of DMNB conjugation was evaluated by increase of their A_{350} signal.

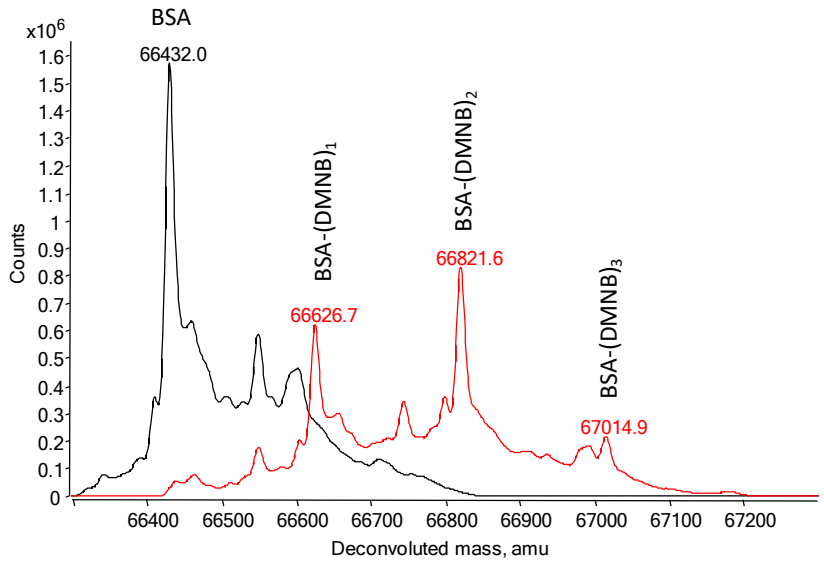

Figure S2. Analysis of the BSA-$(DMNB)_{1-3}$ conjugate by HPLC-ESI/MS (Related to Figure 1).
Three major forms of the BSA-DMNB were formed during the reaction with DMNB bromide indicating number of bound DMNB groups and their respective obtained masses (red line). The BSA-$(DMNB)_{1-3}$ was dialyzed prior loading onto HPLC column. An equal amount of the unlabeled BSA protein (black line) was analyzed for comparison. Corresponding calculated masses (Da) are: 66433 BSA, 66628 BSA-$(DMNB)_1$, 66823 BSA-$(DMNB)_2$, 67018 BSA-$(DMNB)_3$.

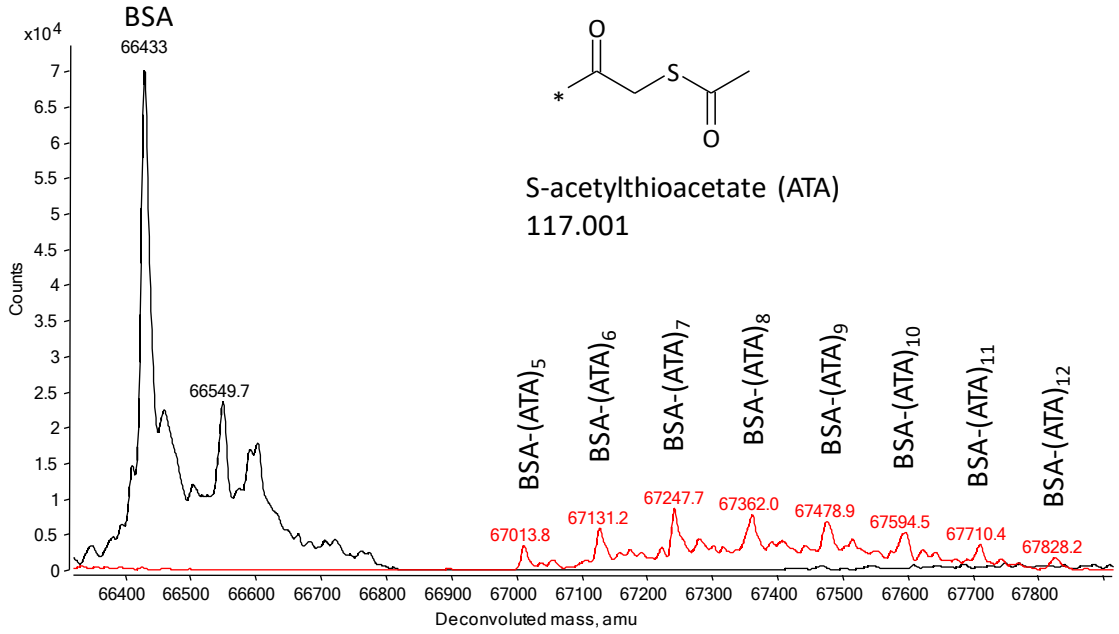

Figure S3. Analysis of the BSA-$(ATA)_{5\text{-}12}$ conjugate by HPLC-ESI/MS (Related to Figure 1).
The BSA protein was reacted with SATA reagent prior to loading onto HPLC column. Major reaction products with varying number of bound ATA groups and their corresponding obtained masses are indicted (red line). An equal amount of the unlabeled BSA protein (black line) was analyzed for comparison. Calculated masses (Da) are: 66433 BSA, 67013 BSA-$(ATA)_5$, 67129 BSA-$(ATA)_6$, 67245 BSA-$(ATA)_7$, 67361 BSA-$(ATA)_8$, 67477 BSA-$(ATA)_9$, 67593 BSA-$(ATA)_{10}$, 67709 BSA-$(ATA)_{11}$, 67825 BSA-$(ATA)_{12}$.

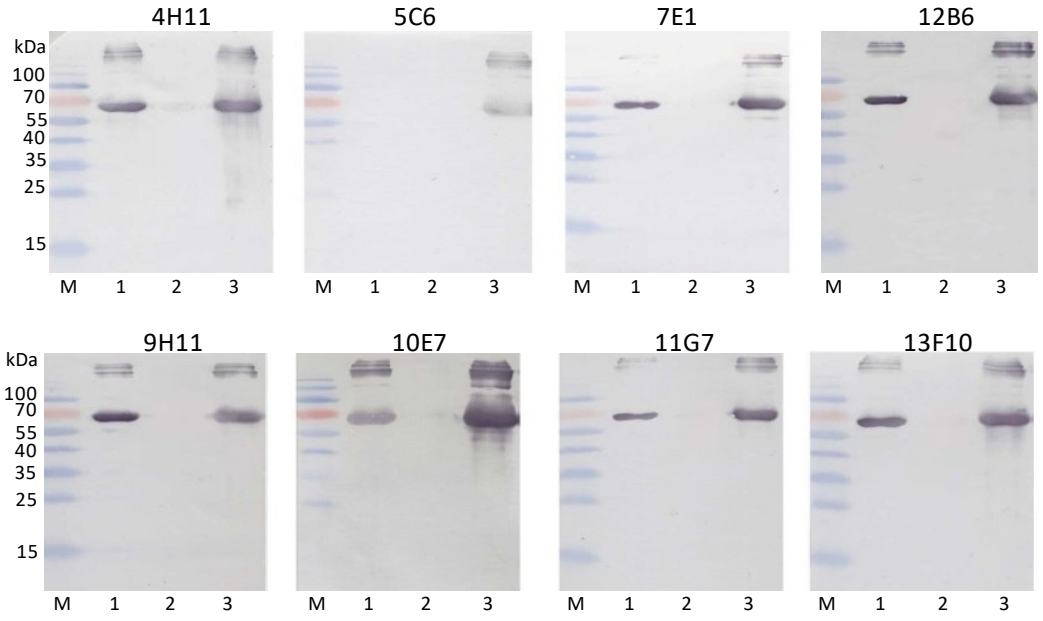

Figure S4. Specificity of the anti-DMNB MAbs produced by eight selected hybridomas (Related to Figure 2 and Table S1).
BSA-$(DMNB)_{1\text{-}3}$ (lane 1) and BSA-AT-(DMNB) (lane 3) antigens were analyzed by western blotting. Unlabeled BSA (lane 2) served as negative control. M, protein size marker.

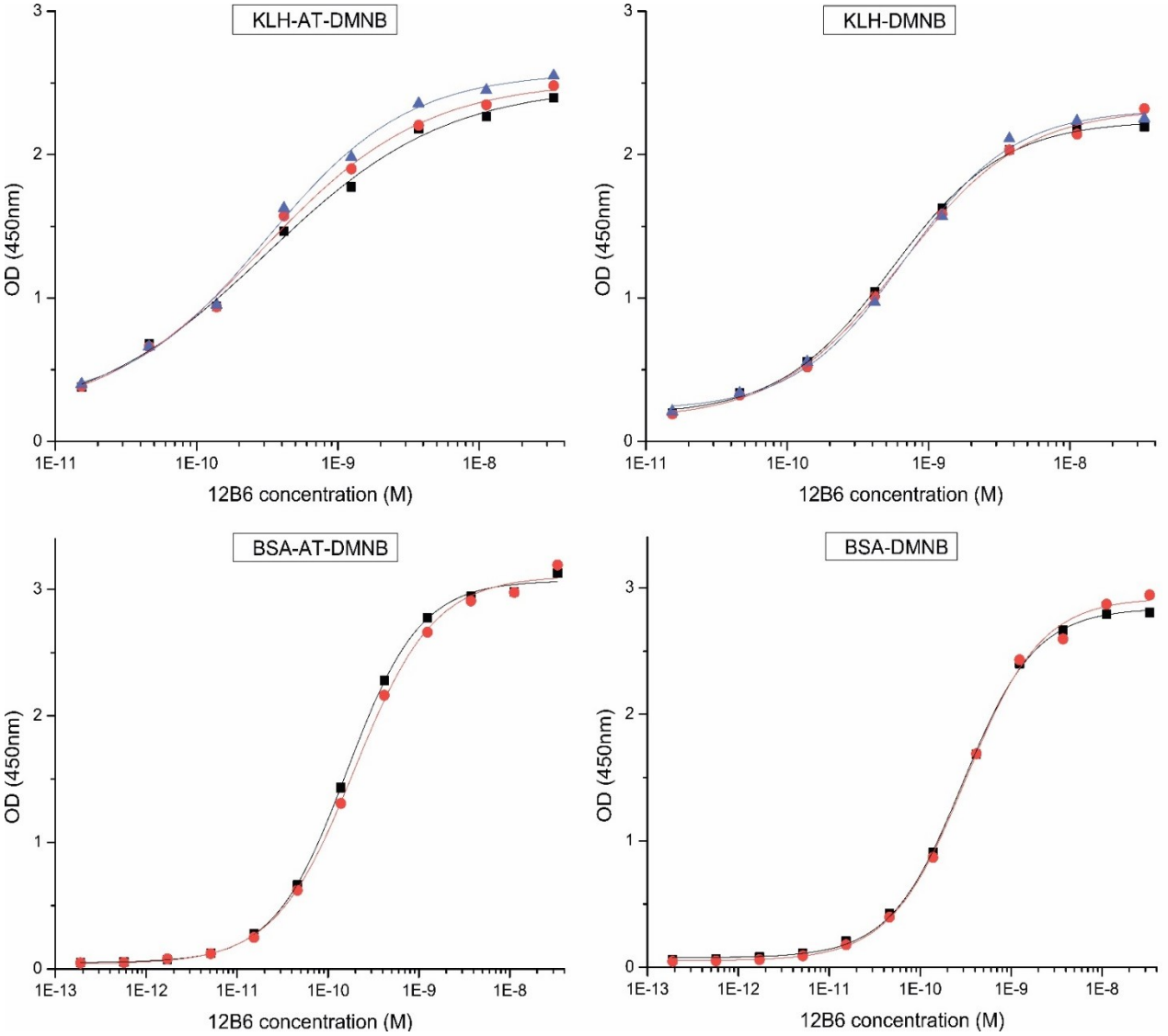

Figure S5. Determination of binding affinity (apparent K_D) of the selected 12B6 antibody (PCSB) to four different antigens using indirect ELISA (Related to Figure 2 and Table S1).

ELISA plates were coated with the indicated DMNB-proteins and various concentrations of primary anti-DMNB antibody 12B6 (PCSB) were used to bind the antigen. Secondary Goat anti-mouse IgG (H+L) – HRP antibodies were used to detect antigen-antibody complexes at a dilution of 1:5000. Signal was developed using TMB and evaluated as optical densities (OD) measured at 450 nm. Titration plots for each replicate are shown as squares, balls and triangles. Apparent dissociation constants K_D were calculated by fitting titration curves to a 4-parameter logistic model using OriginPro 8 (OriginLab) software.

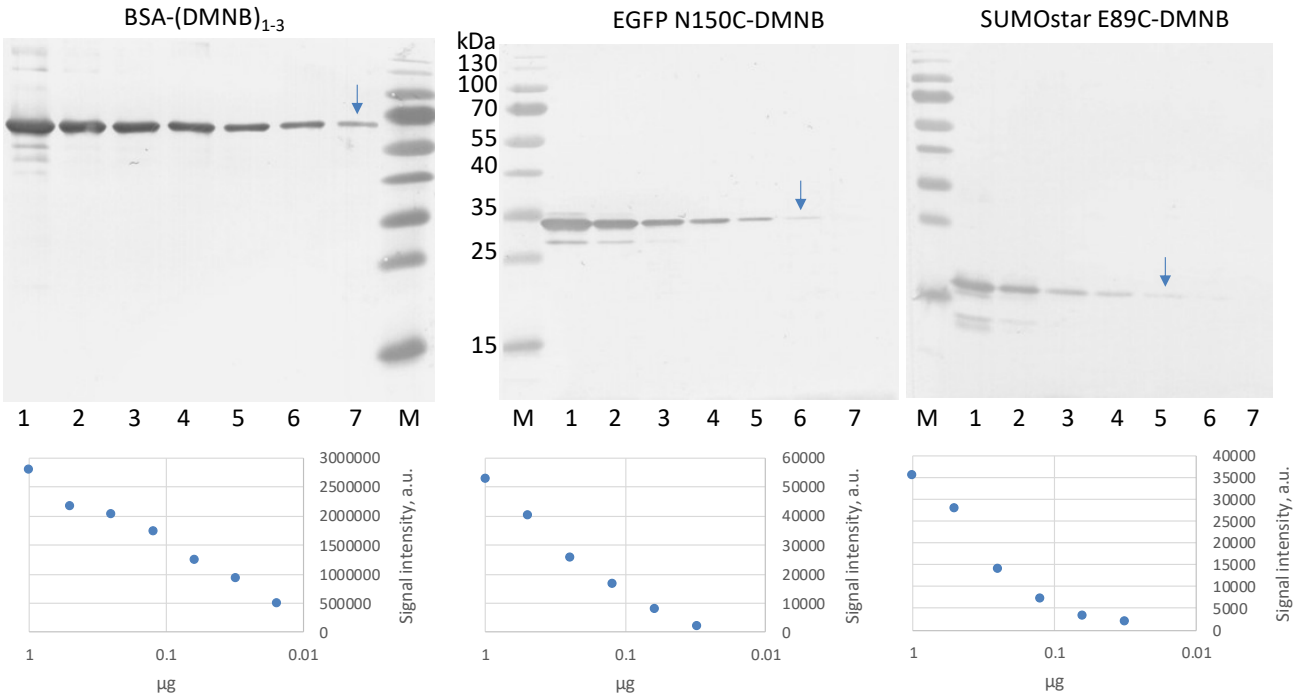

Figure S6. Detection limits of DMNB-proteins by western blotting (Related to Figure 2).
Serial dilutions of purified DMNB-proteins were probed with PCSB. Loaded protein amounts: lane 1, 1000 ng; lane 2, 500 ng; lane 3, 250 ng; lane 4, 125 ng; lane 5, 62.5 ng; lane 6, 31.25 ng; lane 7, 15.625 ng. M, protein size marker. Lower graphs represent plotted band intensities from digitized blots. The smallest detectable concentration is marked by an arrow.

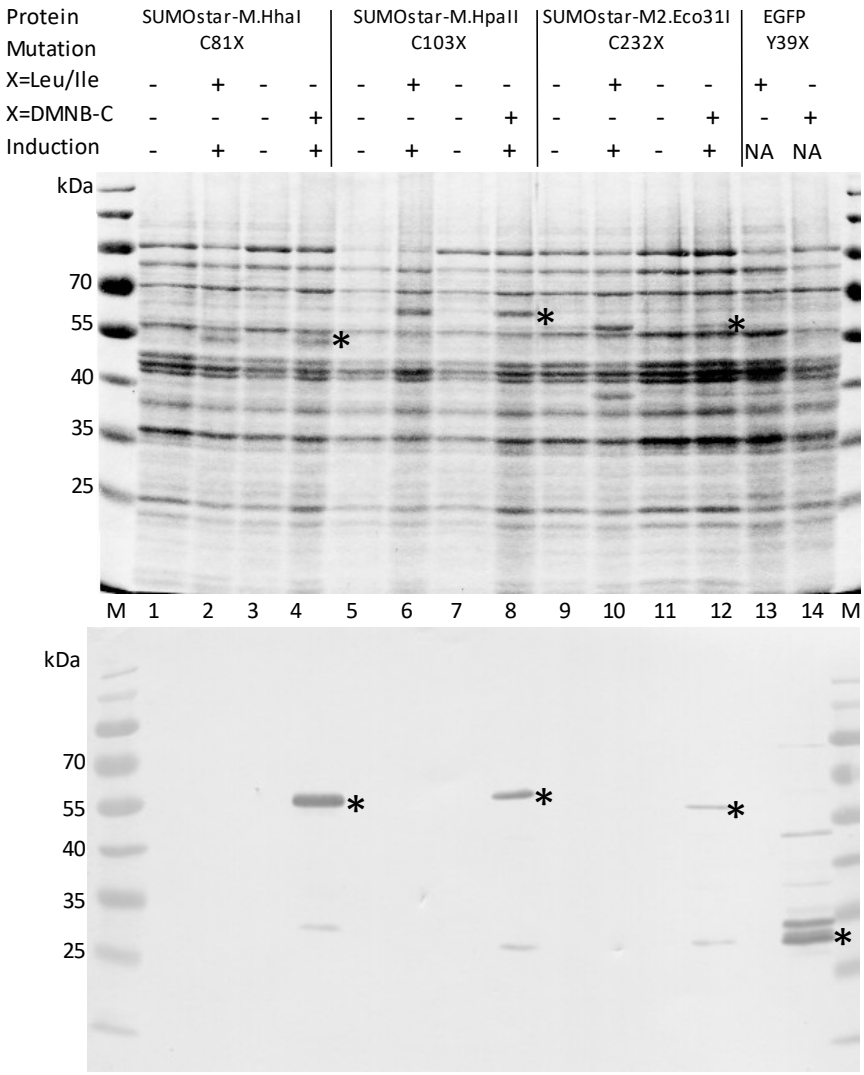

Figure S7. Selective detection of biosynthetic single-label DMNB-proteins in yeast cell lysates by western blotting (Related to Figure 3).

Recombinant proteins containing single DMNB-Cys residues at genetically encoded positions were produced in yeast cells carrying an orthogonal amber-codon suppression system (see Transparent Methods). Uninduced cells or cells encoding Leu/Ile at the same positions served as negative controls. Aliquotes of total cell lysates were fractionated on two parallel SDS-PA gels and visualized by Coomassie staining (top panel) or probed by western blotting using PCSB (bottom panel). Bands of target DMNB-proteins are indicated by asterisks. NA, not applicable (protein was expressed from a constitutive promoter). M, protein size marker.

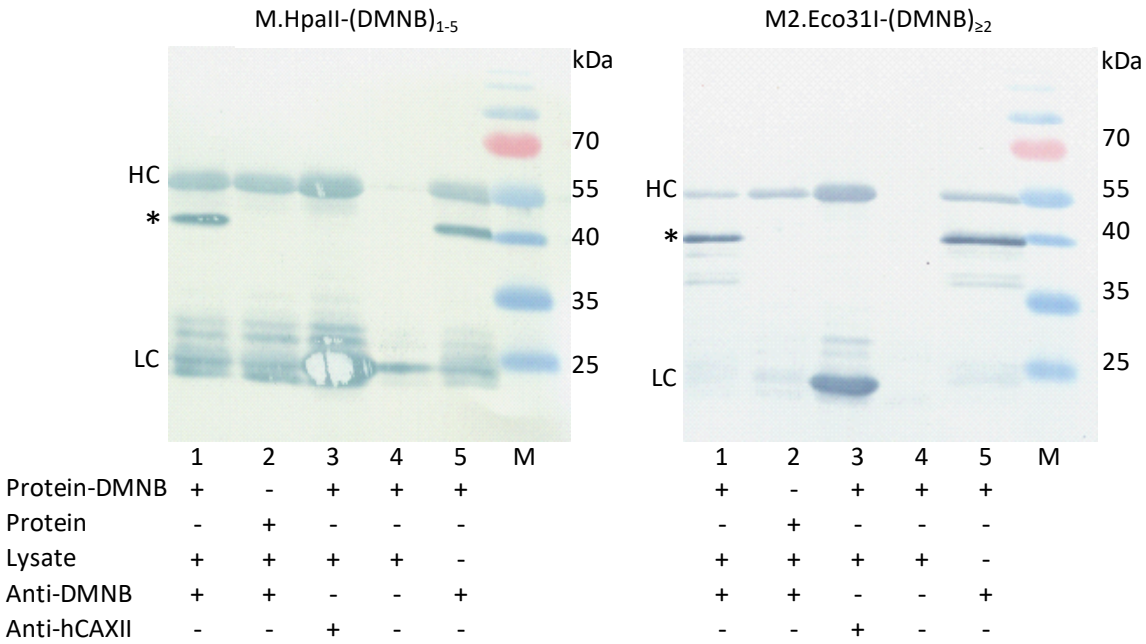

Figure S8. Immunoprecipitation of multi-label DMNB-proteins from complex molecular mixtures (Related to Figure 3).

Immunocomplexes were prepared by first preincubating the Sepharose-Protein A beads with MAbs, washing the beads and further incubating them with DMNB-protein added to a total yeast lysate (lane 1). Control IP reactions contained unlabeled proteins (lane 2), unrelated anti-Human Carbonic Anhydrase XII (anti-hCAXII) MAbs (lane 3), omitted MAbs (lane 4) or omitted lysate (lane 5). The IP complexes were washed, denatured in Laemmli buffer, separated in SDS-PA gel and analyzed by western blotting using PCSB. Recombinant DMNB-proteins are indicated by an asterisk. HC, heavy chain. LC, light chain. M, protein size marker.

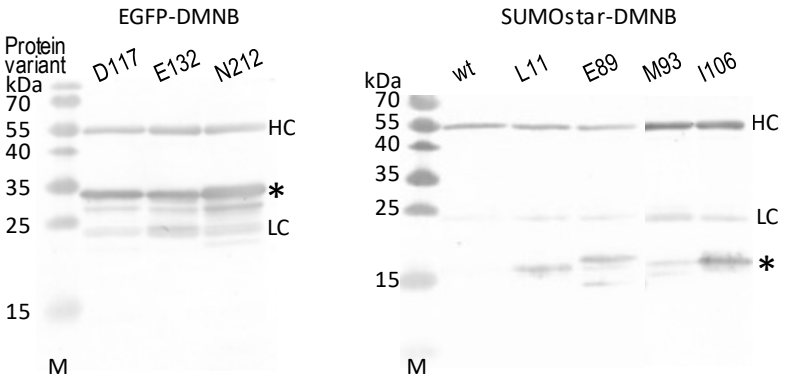

Figure S9. Immuno-capture of chemically DMNB-tagged EGFP and SUMOstar proteins with Cys substitutions placed at selected surface positions (Related to Figure 3).
Target proteins were expressed and purified from *E. coli* cells, treated with DMNB bromide and immunoprecipitated using MagnaBind-Protein A beads preincubated with PCSB. Shown are IP complexes resolved in SDS-PA gel and analyzed by western blotting using PCSB. Bands of DMNB-proteins are indicated by an asterisk. HC, heavy chain. LC, light chain. M, protein size marker.

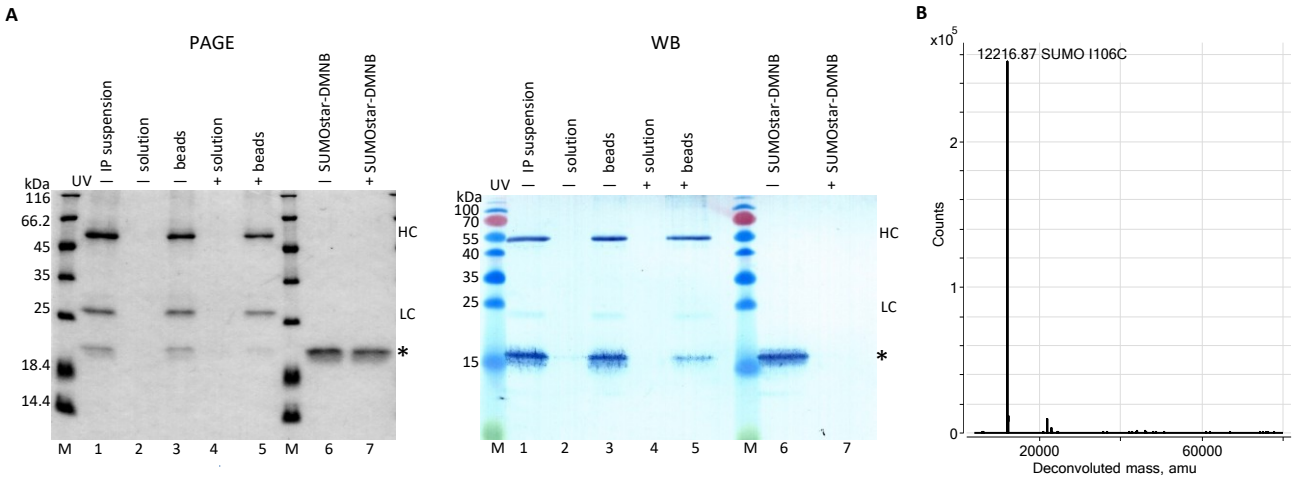

Figure S10. Photochemical release of chemically DMNB-tagged SUMOstar I106C protein from a immunoprecipitation complex (Related to Figure 4).

(A) SDS-PAGE (left panel) and Western blot (right panel) analyses of the IP complexes subjected to photochemical treatment. The SUMOstar I106C-$(DMNB)_{1-2}$ protein was immunocaptured on silica-protein A beads with prebound PCSB (lane 1). The IP complexes were either not exposed (lanes 2, 3) or exposed (lanes 4, 5) to 365 mn light, after which the beads and solution were separated, fractionated in two SDS-PA gels and analyzed by either Coomassie staining (left panel) or western blotting using PCSB (right panel). Control photochemical reactions contained only pure SUMOstar I106C-$(DMNB)_{1-2}$ (lanes 6, 7). Recombinant DMNB-proteins are indicated by an asterisk. HC, heavy chain. LC, light chain. M, protein size standard. (B) Identification of the label-free photolysis product released from IP complexes by HPLC-ESI/MS analysis. Calculated mass: 12216.55 Da; obtained mass: 12216.87 Da. Despite a weak PAGE band visibility of the photolytically released SUMOstar I106C protein in lane 4 (panel A left), its normal abundance is attested by the similar mass spectrometric count (2.5 $x10^5$) as compared to that observed with the biosynthetically caged variant (3 $x10^5$, Fig. 4F, bottom panel).

Supplemental Tables

Table S1. Immunoenzymatic analysis of anti-DMNB MAbs. Related to Figure 2.

MAb	Class and subclass	Apparent *Kd*, M					
		KLH-AT-DMNB	KLH-DMNB	BSA-AT-DMNB	BSA-DMNB	KLH	BSA
4H11	IgG1	9.4×10^{-11}	2.0×10^{-10}	3.6×10^{-10}	2.5×10^{-10}	-	-
5C6	IgG1	-	-	5.9×10^{-9}	-	-	-
7E1	IgG1	5.3×10^{-10}	4.8×10^{-9}	5.5×10^{-10}	1.2×10^{-9}	-	-
9H11	IgG1	3.5×10^{-10}	1.6×10^{-9}	2.3×10^{-10}	9.3×10^{-10}	-	-
10E7	IgG2a	2.3×10^{-10}	3.7×10^{-10}	9.4×10^{-11}	1.7×10^{-10}	-	-
11G7	IgG1	1.3×10^{-12}	2.0×10^{-10}	2.3×10^{-10}	2.9×10^{-10}	-	-
12B6 (PCSB)	IgG2a	4.4×10^{-10}	6.6×10^{-10}	1.8×10^{-10}	3.0×10^{-10}	-	-
13F10	IgG1	2.6×10^{-10}	9.9×10^{-10}	9.8×10^{-11}	3.8×10^{-10}	-	-

- No significant reaction

Table S2. Proteins used in this study. Related to Figures 2, 3 and S7.

	Protein	Variant	Number of photocage groups (n)	Calculated mass	Determined mass	Host organism	Reference
Chemical labeling	KLH	DMNB	ND	ND	ND	commercial preparation	this work
	KLH	AT-DMNB	ND	ND	ND	commercial preparation	this work
	BSA	DMNB	1, 2, 3	66433+195n	66626.7; 66821.6; 67014.9	commercial preparation	this work
	BSA	AT-DMNB	ND	ND	ND	commercial preparation	this work
	M.HpaII	Q104A N335A; DMNB	1, 2, 3, 4, 5	42331.9+195n	42528.35; 42722.42; 42917.85; 43111.71; 43302.89	*E. coli*	this work, (Lukinavičius et al., 2012)
	M2.Eco31I	N127A Q233A; DMNB	≥2	46726.93+195n	47118.0; 47312.92; 47507.9; 47702.5	*E. coli*	this work, (Lukinavičius et al., 2012)
	EGFP	D117C; DMNB	0, 1, 2, 3	28699.29+195n	28699.93; 28894.83; 29089.97; 29285.07	*E. coli*	this work
	EGFP	E132C; DMNB	1, 2, 3	28685.26+195n	28880.75; 29075.85; 29270.9	*E. coli*	this work
	EGFP	N212C; DMNB	0, 1, 2, 3	28700.28+195n	28701.4; 28895.74; 29090.92; 29286.03	*E. coli*	this work
	SUMOstar	DMNB	0, 1	12226.57+195n	12227.09; 12421.98	*E. coli*	this work
	SUMOstar	L11C; DMNB	1, 2	12216.55+195n	12412.36; 12606.84	*E. coli*	this work
	SUMOstar	E89C; DMNB	1, 2	12200.6+195n	12396.28; 12590.96	*E. coli*	this work
	SUMOstar	M93C; DMNB	0, 1	12198.52+195n	12198.96; 12394.08	*E. coli*	this work
	SUMOstar	I106C; DMNB	1, 2	12216.55+195n	12412.23; 12607.27	*E. coli*	this work
Biosynthetic incorporation	EGFP	Y39 C-DMNB	1	28889	28889.32	*S. cerevisiae*	(Rakauskaitė et al., 2015)
	EGFP	Y39 C-MNDPE	1	28887	28887.25	*S. cerevisiae*	this work
	EGFP	Y39 L/I	NA	28704	28704.23	*S. cerevisiae*	(Rakauskaitė et al., 2015)
	EGFP	Y39 U-DMNB	1	28936	28935.5	*S. cerevisiae*	(Rakauskaitė et al., 2015)
	EGFP	D117 C-DMNB	1	28937.34	28937.29	*S. cerevisiae*	this work
	EGFP	E132 C-DMNB	1	28923.31	28923.28	*S. cerevisiae*	this work
	EGFP	N150 C-DMNB	1	28938.33	28938.11	*S. cerevisiae*	this work
	EGFP	N212 C-DMNB	1	28938.33	28938.19	*S. cerevisiae*	this work
	SUMOstar-M.HpaII	C103 C-DMNB	1	52803.5	52804.29	*S. cerevisiae*	(Rakauskaitė et al., 2015)
	SUMOstar-M.HpaII	C103 L/I	NA	52618.4	ND	*S. cerevisiae*	this work
	SUMOstar-M.HhaIΔHT	C81 C-DMNB	1	48921.2	ND	*S. cerevisiae*	this work
	SUMOstar-M.HhaIΔHT	C81 L/I	NA	48679.2	ND	*S. cerevisiae*	this work
	SUMOstar-M2.Eco31I	C232 C-DMNB	1	57198.4	ND	*S. cerevisiae*	this work
	SUMOstar-M2.Eco31I	C232 L/I	NA	57013.4	ND	*S. cerevisiae*	this work
	SUMOstar	wt	NA	12226.57	12226.66	*S. cerevisiae*	this work
	SUMOstar	L11 C-DMNB	1	12411.55	12412.08	*S. cerevisiae*	this work
	SUMOstar	E89 C-DMNB	1	12395.6	12396.32	*S. cerevisiae*	this work
	SUMOstar	M93 C-DMNB	1	12393.52	12394.22	*S. cerevisiae*	this work
	SUMOstar	I106 C-DMNB	1	12411.55	12412.13	*S. cerevisiae*	this work

AT, acetylthio; ND, not determined; NA, not applicable; wt, wild type

Table S3. Inventory of genetic constructs. Related to Figures 3 and S7.

Plasmid ID	Recombinant Protein	Mutation	Promoter	Markers	Host	Reference
pRR64	SUMOstar-M.HpaII	C103Stop	*CUP1*	*URA3 ApR*	*S. cerevisiae*	(Rakauskaitė et al., 2015)
pRR34	SUMOstar-M.HhaI	C81Stop	*CUP1*	*URA3 ApR*	*S. cerevisiae*	This work
pRR60	SUMOstar-M2.Eco31I	C232Stop	*CUP1*	*URA3 ApR*	*S. cerevisiae*	This work
pGFP-TAG	EGFP	Y39Stop	*ADH1*	*LEU2 ApR*	*S. cerevisiae*	(Wang and Wang, 2008)
pRR79	EGFP	D117Stop	*ADH1*	*LEU2 ApR*	*S. cerevisiae*	This work
pRR81	EGFP	E132Stop	*ADH1*	*LEU2 ApR*	*S. cerevisiae*	This work
pRR73	EGFP	N150Stop	*ADH1*	*LEU2 ApR*	*S. cerevisiae*	This work
pRR83	EGFP	N212Stop	*ADH1*	*LEU2 ApR*	*S. cerevisiae*	This work
pRR33	SUMOstar	wt	*CUP1*	*URA3 ApR*	*S. cerevisiae*	This work
pRR75	SUMOstar	L11Stop	*CUP1*	*URA3 ApR*	*S. cerevisiae*	This work
pRR76	SUMOstar	E89Stop	*CUP1*	*URA3 ApR*	*S. cerevisiae*	This work
pRR77	SUMOstar	M93Stop	*CUP1*	*URA3 ApR*	*S. cerevisiae*	This work
pRR78	SUMOstar	I106Stop	*CUP1*	*URA3 ApR*	*S. cerevisiae*	This work
pRR92	EGFP	D117C	P_{BAD}	*ApR*	*E. coli*	This work
pRR93	EGFP	E132C	P_{BAD}	*ApR*	*E. coli*	This work
pRR94	EGFP	N212C	P_{BAD}	*ApR*	*E. coli*	This work
pRR87	SUMOstar	wt	P_{BAD}	*ApR*	*E. coli*	This work
pRR88	SUMOstar	L11C	P_{BAD}	*ApR*	*E. coli*	This work
pRR89	SUMOstar	E89C	P_{BAD}	*ApR*	*E. coli*	This work
pRR90	SUMOstar	M93C	P_{BAD}	*ApR*	*E. coli*	This work
pRR91	SUMOstar	I106C	P_{BAD}	*ApR*	*E. coli*	This work

Transparent Methods

Chemical syntheses

The DMNB-Cys and DMNB-Sec were synthesized as previously described (Rakauskaitė et al., 2015).

Synthesis of MNDPE-Cys was carried out using a modified protocol (Nguyen et al., 2014) from N-Boc-L-cysteine to eliminate unwanted side reactions and to simplify purification which was done using silica chromatography just before removal of Boc protection and thus avoiding expensive reverse-phase purification of the final product.

Analytical TLC was conducted on silica gel plates Silufol 60 F_{254} (Merck) with detection by UV light or a basic potassium permanganate solution. Column chromatography was performed on silica gel (Merck 60Å 230–240 mesh). ^{1}H and ^{13}C NMR spectra were recorded on Bruker Ascend 400 (400 MHz and 100 MHz respectively), chemical shifts are given in ppm. High resolution mass spectra were recorded on Agilent 6230 TOF LC/MS. Melting points were determined in open capillaries using digital melting point IA9100 series apparatus (electrothermal). Solvent evaporation and solution concentration were performed under reduced pressure using a rotary evaporator unless otherwise noted. Unless otherwise indicated, reagents obtained from commercial sources were used without further purification. Solvents were dried and distilled prior to use according to the standard methods.

4,5-(Methylenedioxy)-2-nitroacetophenone

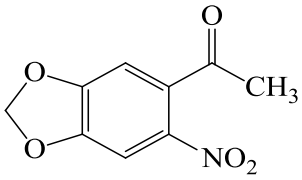

A mixture of HNO_3 (65%; 32 ml) and glacial acetic acid (48 ml) was heated to 50 °C and 3,4-(methylenedioxy) acetophenone (8 g; 487 mmol) solution in glacial acetic acid (24 ml) was added dropwise over 10 minutes maintaining a temperature of 50 °C. Afterwards, the reaction mixture was quickly cooled and poured into ice. The crude product was collected by filtration, washed with water and dried under reduced pressure. An additional portion of the crude product was obtained from filtrate by extraction with dichloromethane (3 × 15 ml). The combined extracts were washed with saturated $NaHCO_3$, dried with anhydrous sodium sulfate and evaporated. Both portions of the crude product were recrystallized from *n*-octane (two times) to obtain the product as yellow crystals.
Yield: 7.19 g (71%); m. p. 110–111 °C.

^{1}H NMR (400 MHz, $CDCl_3$): δ = 7.55 (s, 1H Ar^3-H); 6.76 (s, 1H, Ar^6-H); 6.20 (s, 2H, OCH_2O); 2.50 (s, 3H, CH_3).
^{13}C NMR (100 MHz, $CDCl_3$): δ = 199.2; 152.7; 149.9; 140.2; 135.2; 106.2; 104.8; 103.6; 30.2.

(*R*/*S*)-1-(4',5'-(methylenedioxy)-2'-nitrophenyl)ethanol

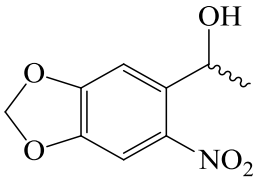

To a solution of 4,5-(methylenedioxy)-2-nitroacetophenone (0.5 g; 2.39 mmol), methanol (2 ml) and DMF (4 ml) cooled to 0 °C sodium borohydride was added in portions of 0.045 g (1.19 mmol) every 30 minutes up to

0.225 g (5.95 mmol). The process was monitored by TLC (chloroform, R_f = 0.10; R_f may be higher if the sample taken from the reaction mixture contains any DMF). On completion, the reaction mixture was quenched with saturated ammonium chloride until the emission of ammonia ceased. The crude product was extracted with diethyl ether (4 × 2 ml), the combined extracts were washed with brine, dried over anhydrous sodium sulfate and the solvent was evaporated. The resulting oil was purified by column chromatography (petrol ether / chloroform - 2:1) to yield the product as a yellow solid.

Yield: 0.455 g (90%); m. p. 84–85 °C.
^{1}H NMR (400 MHz, $CDCl_3$): δ = 7.46 (s, 1H, Ar^3-H); 7.28 (s, 1H, Ar^6-H); 6.13 (s, 2H, OCH_2O); 5.46 (q, ^3J = 6.3 Hz, 1H, CH); 2.46 (s, 1H, OH); 1.54 (d, ^3J = 6.3 Hz, 3H, CH_3).
^{13}C NMR (100 MHz, $CDCl_3$): δ = 152.4; 146.9; 141.5; 139.0; 106.3; 105.1; 102.9; 65.7; 30.2.

(*R*/*S*)-1-bromo-1-[4',5'-(methylenedioxy)-2'-nitrophenyl]ethane

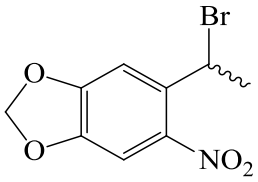

(*R/S*)-1-bromo-1-[4',5'-(methylenedioxy)-2-nitrophenyl]ethane prepared from (*R/S*)-1-(4',5'-(methylenedioxy)-2-nitrophenyl)ethanol as previously reported (Nguyen et al., 2014).
^{1}H NMR (400 MHz, $CDCl_3$): δ = 7.37 (s, 1H, Ar^3-H); 7.29 (s, 1H, Ar^6-H); 6.15 (s, 2H, OCH_2O); 5.91 (q, ^3J = 6.8 Hz, 1H, CH); 2.05 (d, ^3J = 6.8 Hz, 3H, CH_3).

***N*-Boc-L-cysteine**

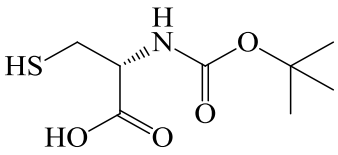

N-Boc-L-cysteine prepared from L-cysteine in two steps using adapted procedures reported previously (Rakauskaitė et al., 2015).

^{1}H NMR (400 MHz, D_2O): δ = 4.28 (br s, 1H CH); 2.93-2.80 (m, 2H, CH_2); 1.35 (s, 9H, CH_3).

***N*-Boc-*S*-{(*R,S*)-1-[4',5'-(methylenedioxy)-2'-nitrophenyl]ethyl}-L-cysteine**

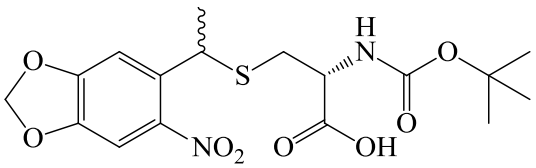

N-boc-L-cysteine (0.139 g; 0.628 mmol), K_2CO_3 (0.182 g; 1.32 mmol) and (R/S)-1-bromo-1-[4',5'-(methylenedioxy)-2-nitrophenyl]ethane (13) (0.258 mg; 0.942 mmol) were dissolved in THF (4.5 ml) and refluxed under an argon atmosphere for 7.5 hours. The reaction was monitored by TLC (toluene / AcOH - 9:1, R_f = 0.35). On completion, the solvent was evaporated, brine (10 ml) was added and the mixture was acidified to pH = 2 with $NaHSO_4$ (1 M). The product was extracted with AcOEt (4 × 5 ml), the combined

extracts were dried over anhydrous sodium sulfate and the solvent was evaporated. The thick oily residue was purified by column chromatography (toluene / AcOH - 25:2, R_f = 0.18) to yield the product as a yellow oil.
Yield: 0.108 g (42%).
^{1}H NMR (400 MHz, $CDCl_3$): δ = 8.36 (s, 1H, COOH); 7.34 & 7.33 (s, 1H, Ar-H); 7.29 & 7.26 (s, 1H, Ar-H); 6.04 & 6.03 (dd, ^2J = 4.4 Hz, 2H, OCH_2O); 5.30-5.15 (m, 1H, NH); 4.75 & 4.72 (q, ^3J = 6.9 Hz, 1H, ArCH); 4.5-4.05 (m, 1H, NCH); 2.91-2.64 (m, 2H, SCH_2); 1.47 & 1.46 (d, ^3J = 6.9 Hz, 3H, CH_3); 1.38 (s, 9H, CH_3).

^{13}C NMR (100 MHz, $CDCl_3$): δ = 175.06 & 174.87; 155.38; 152.02; 146.84; 143.07; 135.73 & 135.52; 107.95; 104.93; 102.95; 80.52; 53.01; 39.59 & 39.42; 33.85 & 33.70; 28.24; 23.08 & 23.05.

_S_-{(_R,S_)-1-[4',5'-(methylenedioxy)-2'-nitrophenyl]ethyl}-L-cysteine trifluoroacetate

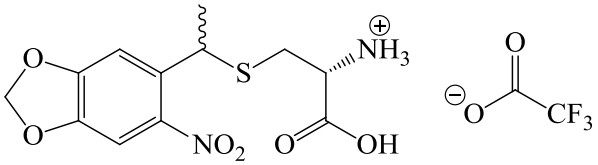

_N_-Boc-S-{(_R,S_)-1-[4',5'-(methylenedioxy)-2-nitrophenyl]ethyl}-L-cysteine (0.108 g; 0.261 mmol) was cooled to 0 °C and TFA (0.5 ml) was added. The mixture was warmed to room temperature and stirred for 25 minutes under an argon atmosphere. Then, dichlorometane (5 ml) was added to the reaction mixture and volatiles were removed with a stream of nitrogen (this step was repeated until no TFA traces were detected in the outgoing stream). The residue was then dissolved in chloroform, diethyl ether was added to the solution and the target product was collected by filtration. The resulting solid was washed with diethyl ether and dried under reduced pressure to yield _S_-{(_R,S_)-1-[4',5'-(methylenedioxy)-2-nitrophenyl]ethyl)-L-cysteine trifluoroacetate as yellow crystals.
Yield: 0.089 mg (79%); 90 °C (dec.).
^{1}H NMR (400 MHz, DMSO-d_6,): δ =7.50 (s, 1H, Ar^3-H); 7.35 & 7.34 (s, 1H Ar^6-H); 6.22 (d, ^2J = 5 Hz, 2H, O-CH_2-O); 4.67 & 4.62 (q, ^3J = 6.8 Hz, 1H, Ar-CH); 3.41-3.32 (m, 1H, NCH); 2.87 & 2.72 (dd, ^3J = 3.3 Hz, ^2J = 13.7 Hz, 1H, C**H**$_a$H$_b$); 2.65-2.55 (m, 1H, CH$_a$**H**$_b$); 1.51 & 1.49 (d, ^3J = 6.8 Hz, 3H, CH_3).
^{13}C NMR (100 MHz, DMSO-d_6): δ = 169.17 & 168.88; 152.13; 147.07; 143.30 & 143.08; 135.27; 108.10; 105.00 & 104.88; 103.81; 53.24; 37.91 & 37.76; 32.94 & 32.64; 22.83.
HRMS: m/z $[M+H]^+$ calcd $[C_{12}H_{14}N_2O_6S+H]$: 315.0645; found 315.0654.

Protein derivatization

The immunization antigen, KLH-AT-DMNB protein, was prepared by first reacting 2 mg of KLH and 40 µg of SATA in a total volume of 200 µl of 100 mM NaH_2PO_4/Na_2HPO_4 pH 7.2, 150 mM NaCl buffer for 30 min at room temperature. The resulted KLH-ATA protein was deacetylated by adding 20 µl of deacetylation solution (0.5 M hydroxylamine and 25 mM EDTA freshly prepared in 20 mM NaH_2PO_4/Na_2HPO_4 pH 7.5, 200 mM NaCl) and incubating for 2 h at room temperature. Reaction product, sulfhydryl-modified protein (KLH-AT), was dialysed against 20 mM NaH_2PO_4/Na_2HPO_4 pH 7.5, 10 mM EDTA, 150 mM NaCl buffer overnight at 4 °C. Next, DMNB bromide was added to a final concentration of 0.5 mM and incubated in dark for 2 h at room temperature. The resulted KLH-AT-DMNB protein was purified by dialysis against 20 mM NaH_2PO_4/Na_2HPO_4 pH 7.5, 150 mM NaCl buffer overnight at 4 °C.

For BSA-AT-DMNB protein preparation, the DMNB-labeling procedure was performed exactly as described for KLH-AT-DMNB, except 1 mg of BSA and 40 µg of SATA in 20 mM KH_2PO_4/K_2HPO_4 pH 7.5, 200 mM KCl were used in first reaction.

The KLH-DMNB protein was prepared by adding 0.5 mM DMNB bromide (final concentration) to 2 mg of KLH protein in 200 µl of 100 mM NaH_2PO_4/Na_2HPO_4 pH 7.2, 150 mM NaCl buffer and incubating in dark for 2 h at room temperature. Unreacted DMNB bromide was removed by dialysis in 20 mM NaH_2PO_4/Na_2HPO_4 pH 7.5, 150 mM NaCl buffer overnight at 4 °C. The BSA-$(DMNB)_{1-3}$, M.HpaII-$(DMNB)_{1-5}$ and M2.Eco31I-$(DMNB)_{\geq 2}$ proteins were prepared by adding 0.5 mM of DMNB bromide (final concentration in no less than 10 fold excess over protein) to BSA, M.HpaII and M2.Eco31I (Lukinavičius et al., 2012) solutions in 20 mM

NaH_2PO_4/Na_2HPO_4 pH 7.5, 200 mM NaCl buffer and incubating in dark for 2 h at room temperature. Unreacted DMNB bromide was removed by dialysis against 5 mM NaH_2PO_4/Na_2HPO_4 pH 7.5, 200 mM NaCl buffer overnight at 4 °C. Mutant variants of EGFP-DMNB and SUMOstar-DMNB proteins were prepared from respective recombinant proteins carrying Cys mutations at indicated positions (Figure 3A). These proteins were isolated from *E. coli* cells and reacted with DMNB bromide. A typical reaction was carried out in 20 mM NaH_2PO_4/Na_2HPO_4 pH 7.5, 200 mM KCl buffer containing no less than 5-fold molar DMNB excess over protein. At first, protein was reduced by adding DTT to a final concentration of 0.1 mM and incubating for 20 min at room temperature. Then, 0.5 mM of DMNB bromide (final concentration) was added and incubated in dark for 2 h at room temperature. Unreacted DMNB bromide was removed by dialysis against 5 mM NaH_2PO_4/Na_2HPO_4 pH 7.5, 200 mM NaCl buffer overnight at 4 °C.

Bacterial, yeast strains and genetic constructs

E. coli DH10B strain was used for genetic cloning and expression of unlabeled EGFP and SUMOstar proteins. Yeast *S. cerevisiae* LWUPF1Δ strain (Wang and Wang, 2008) was a generous gift provided by L. Wang and used to express biosynthetically labeled DMNB-proteins. Plasmids pSNR-LeuRS (Wang and Wang, 2008) and pGFP-TAG (Wang and Wang, 2008) were kind gifts from L. Wang. Plasmid pRR6 was constructed earlier (Rakauskaitė et al., 2015).

Plasmids for genetic DMNB-Cys incorporation into proteins SUMOstar-M.HhaI and SUMOstar-M2.Eco31I at their catalytic residues C81 and C232 respectively were made as previously described for SUMOstar-M.HpaII (pRR64) construct (Rakauskaitė et al., 2015). Specifically, the M.HhaI and M2.Eco31I genes were PCR-amplified from their corresponding plasmids pΔ324GH6 (Gerasimaitė et al., 2009) and pET15b-eco31I (Lukinavičius et al., 2012) and cloned to pY-SUMOstar vector (LifeSensors) fusing to a SUMOstar gene according to manufacturer's recommendations. Amber stop codon mutations C81TAG and C232TAG in the fusion SUMOstar-M.HhaI and SUMOstar-M2.Eco31I genes, respectively, were introduced by PCR-based site directed mutagenesis (SDM) using Phusion High-Fidelity DNA polymerase (ThermoFisher Scientific). The selective *TRP*1 marker in both constructs was replaced with the *URA*3 marker from pRR64 using standard PCR cloning.

For biosynthetic DMNB-Cys incorporation at selected locations of EGFP, the wild-type TAC codon at the Y39 position of the pGFP-TAG plasmid was restored and new TAG codon substitutions were placed at the D117, E132, N150, N212 positions using SDM.

For DMNB-SUMOstar protein expression a modified pY-SUMOstar vector (LifeSensors) was used. The original *TRP1* marker was replaced with the *URA3* marker from plasmid pRR64 employing standard genetic engineering techniques and TAG codons at positions L11, E89, M93, I106 in a SUMOstar gene were introduced by SDM.

For expression of EGFP and SUMOstar proteins in *E. coli* cells, the respective genes were cloned under pBAD promoter (Guzman et al., 1995). Cysteine (TGT codon) substitutions were introduced by SDM at positions D117, E132, N212 and positions L11, E89, M93, I106 of EGFP and SUMOstar genes respectively.

All new constructs were verified by sequencing and are listed in Table S3.

Protein production and purification

Mutant Cys variants of recombinant proteins EGFP and SUMOstar used in chemical labeling reactions were expressed in *E. coli* DH10B cells and purified according to standard Ni-IMAC procedure using His SpinTrap™ columns (GE Healthcare) and following manufacturer's recommendations.

Recombinant proteins containing single DMNB-tagged residues at genetically encoded positions were produced by biosynthetic incorporation of DMNB-Cys in *S. cerevisiae* cells carrying an orthogonal amber-codon suppression system (Rakauskaitė et al., 2015). Specifically, for DMNB-EGFP protein production, yeast cells were co-transformed with pRR6 plasmid (Rakauskaitė et al., 2015) carrying *Ec*tRNA$^{\mathrm{Leu}}_{\mathrm{CUA}}$ and LeuRSBH5T252A genes (Lemke et al., 2007) and one of the pGFP-TAG, pRR79, pRR81, pRR73 or pRR83 plasmids carrying EGFP genes with respective amber mutations (Table S3). Transformants were selected and further cultivated in synthetic drop-out medium lacking Leu and Trp at 30 °C with 220 rpm shaking.

Exponentially growing cells were collected, resuspended in 0.25 volume of selective medium containing 2 mM DMNB-Cys and incubated overnight in the dark at 30 °C with 220 rpm shaking. Cells were collected, washed with water, lysed with Y-PER reagent (Thermo Scientific) and recombinant proteins were isolated using unpacked Chelating Sepharose Fast Flow (GE Healthcare) charged with Ni^{2+} according to manufacturer's instructions. Amicon Ultra 10K centrifugal filter units (Merck Millipore) were used to exchange buffer and concentrate samples. Proteins were aliquoted and stored in 20 mM KH_2PO_4/K_2HPO_4 pH 7.4, 200 mM KCl at -80 °C. For EGFP Y39 C-MNDPE protein expression, 2 mM MNDPE-Cys instead of DMNB-Cys was added to yeast growth medium.

For DMNB-SUMOstar protein production, yeast cells were co-transformed with pRR6 plasmid and one of the pRR33, pRR75, pRR76, pRR77, or pRR78 plasmids carrying SUMOstar gene with respective amber mutation (Table S3). Transformants were selected and further cultivated in synthetic drop-out medium lacking uracil and Trp at 30 °C with 220 rpm shaking. Exponentially growing cells were collected, resuspended in 0.25 volume of selective medium containing 2mM DMNB-Cys and 100 µM $CuSO_4$ and incubated in the dark tor 5 hours at 30 °C with 220 rpm shaking. Cells were collected, washed with water, lysed applying the Y-PER reagent and DMNB-SUMOstar proteins were isolated using His-Select spin columns (Sigma-Aldrich) as described by manufacturer. Amicon Ultra 3K centrifugal filter units (Merck Millipore) were used to exchange buffer and concentrate samples. Proteins were aliquoted and stored in 20 mM KH_2PO_4/K_2HPO_4, pH 7.4, 200 mM KCl at -80 °C.

Recombinant DMNB-SUMOstar-MTases (Figure S7) were expressed by co-transforming yeast cells with pRR6 and one of the pRR64, pRR34, or pRR60 plasmids carrying SUMOstar-MTase fusion genes with amber codon replacement for catalytic Cys (Table S3). Transformants were selected and further cultivated in synthetic drop-out medium lacking uracil and Trp at 30 °C with 220 rpm shaking. Exponentially growing cells were collected, resuspended in 0.25 volume of selective medium containing 2 mM DMNB-Cys and 100 µM $CuSO_4$ and incubated in the dark tor 5 hours at 30 °C with 220 rpm shaking. Cells were collected, washed with water, resuspended in 0.1 M NaOH and incubated at room temperature for 10 min. Cells were collected, mixed within SDS-PAGE loading buffer and heated at 95 °C for 10 min prior to SDS-PAGE analysis. Control cultures expressing SUMOstar-MTases with Leu/Ile substitutions for catalytic Cys were made by co-transforming yeast cells with pSNR-LeuRS carrying *Ec*tRNA$^{\mathrm{Leu}}_{\mathrm{CUA}}$ and LeuRS genes (Wang and Wang, 2008) and one of the pRR64, pRR34, or pRR60 plasmids. Cells were treated exactly as the ones expressing DMNB-SUMOstar-MTases, except the DMNB-Cys was omitted from the growth medium. Control uninduced cultures were grown without $CuSO_4$.

Cells expressing recombinant EGFP Y39C-DMNB or EGFP Y39L/I protein (Figure S7) were generated by co-transforming yeast cells with pEGFP-TAG and pRR6 or pSNR-LeuRS, respectively. Transformants were selected and further cultivated in synthetic drop-out medium lacking Leu and Trp at 30 °C with 220 rpm shaking. Exponentially growing cells were collected, resuspended in 0.25 volume of selective medium containing 2 mM DMNB-Cys and incubated overnight in the dark at 30 °C with 220 rpm shaking. For SDS-PAGE analysis cells were processed as described for DMNB-SUMOstar-MTases. Total yeast cell lysates (Figure S8) were made using glass beads method (Sattlegger et al., 2011) from yeast *S. cerevisiae* LWUPF1Δ cells exponentially growing in SC medium. For other IP experiments, yeast cells expressing DMNB-proteins were lysed with Y-PER reagent (Thermo Scientific).

Protein analysis

The identity of purified proteins (Table S2) and their photo-decaging products were confirmed by HPLC/ESI-MS analysis. Samples were analyzed on an integrated HPLC/ESI-MS system (Agilent 1290 Infinity) equipped with a Poroshell 300SB-C8 column (2.1x75 mm, 5 µm) by elution with a linear gradient of solvents A (1% formic acid in water) and B (1% formic acid in acetonitrile) at a flow rate of 0.4 ml/min at 30 °C as follows: 0–1 min, 2% B; 1–6 min, 2–98% B; 6–7 min, 98% B; 7–9 min, 98–2% B; 9–10 min, 2% B. High-resolution mass spectra of protein products were acquired on an Agilent Q-TOF 6520 mass analyzer (100–3200 m/z range, positive ionization mode). The results were analyzed with Agilent MassHunter Qualitative Analysis software. Protein mass spectra were deconvoluted (maximum entropy) in the range of 4,000–80,000 Da. Theoretical mass values were obtained using ProtParam tool (*web.expasy.org/protparam/*) with manual adjustments for EGFP chromophore formation (Ormö et al., 1996).

PyMOL models of EGFP and SUMO proteins were built using deposited crystallographic coordinates (PDB codes 2Y0G (Royant and Noirclerc-Savoye, 2011) and 1L2N (Sheng and Liao, 2002) respectively.

Generation of antibodies

Subcutaneous injections to 3 BALB/c female mice (6-8 weeks of age) were performed 3 times every 28 days and consisted of 50 µg of DMNB-AT-KLH antigen mixed with complete Freund's adjuvant, incomplete Freund's adjuvant or PBS for the first, second and third immunization, respectively. ELISA was performed to evaluate DMNB-specific antibody titer in mice tail blood samples collected before each immunization. Spleen cells from the high responder mouse were fused with mouse myeloma Sp2/0 cells, resulting hybridomas were selected by cultivation in HAT medium and screened by ELISA for hybrid cell clones producing DMNB-specific antibodies (Table S1). Hybridomas were frozen in cryopreservation medium and placed in liquid nitrogen for long-term storage. Antibodies were isotyped using Mouse Immunoglobulin Isotyping ELISA Kit (BD Pharmingen), and their apparent dissociation constants were determined by indirect ELISA (Liliom et al., 1991). The selected anti-DMNB MAbs produced by 12B6 hybridoma cells were affinity purified using Protein A Sepharose (HiTrap Protein A HP 1 ml column, GE Healthcare) following manufacturers procedure.

Western blot analysis

Protein samples for western blotting were mixed within Laemmli buffer, heated at 95 °C for 10 min and resolved by electrophoresis on a 15% SDS-PA gel. Proteins were transferred to a PVDF (GE Healthcare) membrane and after blocking overnight at 4 °C with Roti-Block solution (Roth) probed with anti-DMNB antibodies diluted in Roti-Block solution (1 µg/ml concentration for purified antibodies or 1:10 dilution for hybridoma growth medium) for 1 h at room temperature. Bound antibodies were detected with secondary goat anti-mouse IgG (H+L) labelled with HRP (Bio-Rad) diluted 1:4000 in Roti-Block solution by incubating for 1 h at room temperature. Immunocomplexes were visualized using 1-Step™ Ultra TMB-ELISA Substrate Solution (Thermo Scientific) reagent according to manufacturer's instructions.

Immunoprecipitation

The immunoprecipitation complexes were assembled on a Sepharose-Protein A (GE Healthcare), MagnaBind-Protein A (Thermo Scientific) or 1 µm Silica-Protein A (Kisker-Biotech) beads. Beads were prewashed 2 times with PBS and, typically, 50 µl of beads solution were incubated with 100 µg of 12B6 MAbs in a total volume of 200 µl PBS at room temperature for 1 h with rotation. Beads were then rinsed with PBS and incubated with PBS containing 1% BSA (GE Healthcare). The amount of bound MAbs were determined by A_{280} measurements approximately yielding 30 µg antibodies bound to 50 µl of beads suspension. A purified DMNB-protein in PBS (≥1.5-fold molar excess over bound MAbs) or clarified total yeast cell lysate with an expressed DMNB-protein (1:10 dilution in PBS) was next added to the prepared beads in a total volume of 200 µl or 400 µl respectively and incubated with rotation in the dark at room temperature for 1 h. Beads were washed once with and resuspended in PBS containing 2 mM DTT.

Photolytic decaging

IP complexes were assembled using Silica-Protein A beads resuspended in PBS buffer containing 10 mM L-methionine (Kerwin and Remmele, 2007). 65 µl of sample solution was placed in a cap cut from a Protein LoBind tube (Eppendorf) mounted on an ice-cold mirror. Samples were illuminated at a surface area of 0.8 cm^2 for 10 min with an optical power of 6.2 mW produced by a 365 nm top-mounted LED light source.

Fluorescence measurements

Fluorescence intensities of EGFP solutions separated from IP complexes before and after UV treatment were measured using microplate reader Synergy H4 (BioTek).

Fluorescence of IP complexes containing EGFP-DMNB proteins was visualized using EVOS FL Auto Imaging System (Invitrogen). Ten µl of bead suspension before and after UV exposure was placed in Burker's counting chamber (Fisher Scientific) and observed using 20X objective (scale bar 200 µm). Images were taken using EVOS™ Light Cube, GFP (Invitrogen).

Fluorescence of the IP complexes carrying EGFP-DMNB proteins was quantified by flow cytometry. Twenty µl of beads suspension was diluted 1:38.5 in PBS containing 0.1% Tween-20 (Roth) and 1% FBS (Biochrom)

and measured using a flow cytometer. Flow cytometric data was acquired on a CyFlow Space flow cytometer (Sysmex Partec) and analysed using FlowJo software (FlowJo, LLC).

Supplemental references

Gerasimaitė, R., Vilkaitis, G., and Klimašauskas, S. (2009). A directed evolution design of a GCG-specific DNA hemimethylase. Nucleic Acids Res *37*, 7332-7341.

Guzman, L.M., Belin, D., Carson, M.J., and Beckwith, J. (1995). Tight regulation, modulation, and high-level expression by vectors containing the arabinose PBAD promoter. J Bacteriol *177*, 4121-4130.

Kerwin, B.A., and Remmele, R.L., Jr. (2007). Protect from light: photodegradation and protein biologics. J Pharm Sci *96*, 1468-1479.

Liliom, K., Orosz, F., Horváth, L., and Ovádi, J. (1991). Quantitative evaluation of indirect ELISA. Effect of calmodulin antagonists on antibody binding to calmodulin. J Immunol Methods *143*, 119-125.

Lukinavičius, G., Lapinaitė, A., Urbanavičiūtė, G., Gerasimaitė, R., and Klimašauskas, S. (2012). Engineering the DNA cytosine-5 methyltransferase reaction for sequence-specific labeling of DNA. Nucleic Acids Res *40*, 11594-11602.

Ormö, M., Cubitt, A.B., Kallio, K., Gross, L.A., Tsien, R.Y., and Remington, S.J. (1996). Crystal Structure of the Aequorea victoria Green Fluorescent Protein. Science, *273,*1392-1395.

Rakauskaitė, R., Urbanavičiūtė, G., Rukšėnaitė, A., Liutkevičiūtė, Z., Juškėnas, R., Masevičius, V., and Klimašauskas, S. (2015). Biosynthetic selenoproteins with genetically-encoded photocaged selenocysteines. Chem Commun *51*, 8245-8248.

Royant, A., and Noirclerc-Savoye, M. (2011). Stabilizing role of glutamic acid 222 in the structure of Enhanced Green Fluorescent Protein. J Struct Biol *174*, 385-390.

Sattlegger, E., Visweswaraiah, J., and Dautel, M. (2011). Generating highly concentrated yeast whole cell extract using low-cost equipment. Protoc Ex, DOI: 10.1038/protex.2011.1212.

Sheng, W., and Liao, X. (2002). Solution structure of a yeast ubiquitin-like protein Smt3: the role of structurally less defined sequences in protein-protein recognitions. Protein Sci *11*, 1482-1491.